

# Comparison of dopamine release and uptake parameters across sex, species and striatal subregions

Lindsey B. Kuiper<sup>1</sup>  | Monica H. Dawes<sup>1</sup>  | Alyssa M. West<sup>1</sup> |  
 Emily K. DiMarco<sup>1</sup>  | Emma V. Galante<sup>1</sup> | Kenneth T. Kishida<sup>1,2,3</sup>  |  
 Sara R. Jones<sup>1</sup> 

<sup>1</sup>Department of Translational Neuroscience, Wake Forest University School of Medicine, Winston-Salem, North Carolina, USA

<sup>2</sup>Department of Biomedical Engineering, Wake Forest University School of Medicine, Winston-Salem, North Carolina, USA

<sup>3</sup>Department of Neurosurgery, Wake Forest University School of Medicine, Winston-Salem, North Carolina, USA

## Correspondence

Sara R. Jones, Department of Translational Neuroscience, 1 Medical Center Boulevard, Wake Forest University School of Medicine, Winston-Salem, NC 27157, USA.

Email: [srjones@wakehealth.edu](mailto:srjones@wakehealth.edu)

## Funding information

National Institute on Drug Abuse, Grant/Award Numbers: F31 DA057815, P50 DA006634, R01 DA048096, R01 DA048490, R01 DA054694, T32 DA041349; National Institute on Alcohol Abuse and Alcoholism, Grant/Award Numbers: P50 AA026117, T32 AA007565, U01 AA014091; National Institute of Mental Health, Grant/Award Numbers: R01 MH121099, R01 MH124115; National Center for Advancing Translational Sciences, Grant/Award Number: KL2 TR001420

Edited by: Yoland Smith

**Abbreviations:** CFM, carbon fibre microelectrode; CINs, cholinergic interneurons; DA, dopamine; DAT, dopamine transporter; dlCPu, dorsolateral caudate putamen; DT, difference threshold; FSCV, fast-scan cyclic voltammetry; lshell, lateral shell; mshell, medial shell; NAc, nucleus accumbens; nAChRs, nicotinic acetylcholine receptors; S/N, signal-to-noise; SIR, stimulation intensity-response; vmCPu, ventromedial caudate putamen; VTA, ventral tegmental area.

L.B. Kuiper and M.H. Dawes contributed equally to this work.

## Abstract

For over four decades, fast-scan cyclic voltammetry (FSCV) has been used to selectively measure neurotransmitters such as dopamine (DA) with high spatial and temporal resolution, providing detailed information about the regulation of DA in the extracellular space. FSCV is an optimal method for determining concentrations of stimulus-evoked DA in brain tissue. When modelling diseases involving disturbances in DA transmission, preclinical rodent models are especially useful because of the availability of specialized tools and techniques that serve as a foundation for translational research. There is known heterogeneity in DA dynamics between and within DA-innervated brain structures and between males and females. However, systematic evaluations of sex- and species-differences across multiple areas are lacking. Therefore, using FSCV, we captured a broad range of DA dynamics across five sub-regions of the dorsal and ventral striatum of males and females of both rats and mice that reflect the functional heterogeneity of DA kinetics and dynamics within these structures. While numerous differences were found, in particular, we documented a strong, consistent pattern of increased DA transporter activity in females in all of the regions surveyed. The data herein are intended to be used as a resource for further investigation of DA terminal function.

## KEY WORDS

caudate putamen, fast-scan cyclic voltammetry, nucleus accumbens, rodents, sex differences

## 1 | INTRODUCTION

Fast-scan cyclic voltammetry (FSCV) is a fundamental tool used to measure monoamine neurotransmitters, including dopamine (DA). In brain slice preparations, FSCV is an effective way to elucidate the properties of synaptic regulation of DA under tightly controlled experimental conditions. This is especially useful in assessing the properties of the DA synapse, providing valuable insight into disease mechanisms involving DA dysregulation. Here, we centre our discussion on the striatum, a collection of loci where DA exerts a major influence on behavioural output. In addition, we turn our attention to the laboratory rat and mouse, each of which is a valuable model system with unique phenotypic characteristics that are used to model aspects of human psychiatric disease. Importantly, these rodent models afford robust throughput for techniques such as FSCV.

The rodent striatum, principally comprised of GABAergic medium spiny neurons, receives DA signals from sets of distinct, but highly heterogeneous, clusters of DAergic neurons in the midbrain. These DAergic afferents project along the nigrostriatal (dorsal) and mesolimbic (ventral) pathways, which are involved in motor control and motivated behaviour, respectively (Gonzales & Smith, 2015; Mohebi et al., 2019). Upon engagement of these pathways, the resulting DA transmission in the striatum is a key component of appropriating movement either towards or away from salient stimuli. Survival of the organism depends on the adequate function of this system. Several synaptic proteins, notably the DA transporter (DAT) and autoreceptors, regulate DA transmission. These and other regulatory mechanisms are thoroughly reviewed (Nolan et al., 2020; Zachry et al., 2021), though many dynamic properties of the DA system are not yet fully understood. Ex vivo FSCV has helped shape much of the current understanding of DA dynamics, and the technique continues to be an indispensable means of linking disruptions in DA transmission with specific maladaptive behaviours.

A unique advantage of FSCV in conjunction with controlled pulses of electrical stimulation is that the experimenter can adjust stimulation parameters to mimic the physiological firing rates of DA neurons. DA neurons exhibit both tonic and phasic firing patterns, with tonic firing associated with basal conditions (Floresco, 2007), which are best modelled in deafferented striatum (slices) by applying single pulses of stimulation or multiple pulses at low frequencies. The experimenter also has the flexibility to vary the stimulation intensity of each pulse through modulation of the stimulating current applied, and though this technique has not been widely used, it has the potential to provide even more information about

the synaptic environment (we will explore this in the present study). When analysed on the subsecond timescale afforded by FSCV, DA evoked by each stimulation can be modelled using Michaelis–Menten-based kinetics to assess DA release and clearance, or uptake, via DATs (Ferris, Calipari, Yorgason, & Jones, 2013). In addition to this high temporal resolution, FSCV recordings in brain slices prepared from rodents can be performed with both high spatial resolution and the ability to readily target small subnuclei within brain structures, an ability that is limited when targeting deep brain structures *in vivo*.

Previous studies using *ex vivo* FSCV have highlighted variations in DA dynamics between striatal brain regions (Garris et al., 1994; Garris & Wightman, 1994; Jones et al., 1995, 1996; Saddoris et al., 2015; Wightman et al., 1988) or changes in DA dynamics within the same brain region resulting from environmental factors such as natural diurnal rhythms (Ferris et al., 2014; Jameson et al., 2023) and exposure to psychotropic drugs (Budygin et al., 2007; Ferris, Calipari, Melchior, et al., 2013; George et al., 2022). Such studies lay the groundwork for theories related to the involvement of DA in psychiatric illness. Other studies have highlighted sex differences in DA release and uptake (reviewed in Zachry et al., 2021), which may, at least in part, explain the appearance of wide-ranging discrepancies in the development of DA-related psychiatric illness between men and women (Christiansen et al., 2022). To provide a unifying framework for these observations, which have been made across laboratories, model systems and experimental conditions, we conducted a single study to examine DA function across anatomically defined subregions of the striatum in male and female mice and rats with an array of stimulation intensities.

A primary goal of the present work was to generate an openly accessible database of systematic FSCV measurements across the rodent striatum. DA release events evoked by single pulses of stimulation are used to examine the dynamics of tonic DA neuron activity in the striatum (Ferris, Calipari, Yorgason, & Jones, 2013; Rice et al., 2011). It is known that electrically evoked DA signals vary as much, if not more, within the same target brain region as between animals (Lucio Boschen et al., 2021). With this in mind, all discernable DA signals are included in the dataset to capture the full distribution of measurable DA signals from the following subdivisions of dorsal and ventral striatum: dorsolateral caudate putamen (dlCPu), ventromedial caudate putamen (vmCPu), nucleus accumbens (NAc) core (core), NAc lateral shell (lshell) and NAc medial shell (mshell). We also characterize the dynamic properties of DA terminals using measurements of evoked DA concentration as a function of applied stimulation current, here termed the stimulus

intensity-response (SIR) curve. Finally, DA researchers can use this openly available dataset to perform hypothesis-driven research or as a training tool in the analysis of multivariate data. We provide a graphical overview of all included data, with an emphasis on sex as a biological variable.

## 2 | MATERIALS AND METHODS

### 2.1 | Animals

Male and female C57BL/6J mice (8–10 weeks old; Jackson Laboratories, Bar Harbor, ME) were maintained on a 12:12 h light/dark cycle (6:00 AM on; 6:00 PM off) with ad libitum food and water. Male and female Sprague-Dawley rats (350–400 g; Envigo, Indianapolis, IN) were maintained on a 12:12 h light/dark cycle (6:00 AM on; 6:00 PM off) with ad libitum food and water. All experiments were performed during the animals' light cycle. All animals were maintained according to the National Institutes of Health guidelines in Association for Assessment and Accreditation of Laboratory Animal Care accredited facilities. The experimental protocol was approved by the Institutional Animal Care and Use Committee at Wake Forest University School of Medicine.

### 2.2 | Brain slice preparation

Animals were deeply anesthetized using isoflurane gas in an induction chamber prior to being rapidly decapitated. The brain was removed and placed into ice-cold, pre-oxygenated artificial cerebrospinal fluid (aCSF; 126 mM NaCl, 2.5 mM KCl, 1.2 mM NaH<sub>2</sub>PO<sub>4</sub>, 2.4 mM CaCl<sub>2</sub>, 1.2 mM MgCl<sub>2</sub>, 25 mM NaHCO<sub>3</sub>, 11.0 mM glucose and 0.4 mM L-ascorbic acid). A vibratome (Leica Biosystems, Buffalo Grove IL, USA) was used to prepare coronal brain slices (mouse: 300 µm thick, rat: 400 µm thick) containing the striatum. All slices were transferred to recording chambers and incubated at 32°C in oxygenated aCSF for at least 1 h prior to experimental manipulations.

### 2.3 | Approximation of estrous stage

The estrous stage was not monitored in any of the females. However, post-mortem vaginal lavage was performed to approximate the estrous stage for each female. This approximation was not used as a covariate in any of our analyses, but it was recorded for potential future exploratory analysis. Samples of vaginal epithelial cells were prepared for cytology by flushing saline

(approximately 0.1 mL for mice and 0.2 mL for rats) via a glass pipette into the vaginal canal 2–3 times and then placing a small drop of the sample onto a glass slide. Without staining, samples were evaluated on a light microscope under low magnification (10×) using the criteria detailed in Cora et al. (2015).

### 2.4 | Study design

The study was not pre-registered and was exploratory. A total of 24 animals were included in this study, with six animals each per sex and species. Experiments began at 8:00–9:00 AM, and recordings lasted until 6:00–8:00 PM. A single mouse and rat were run simultaneously on the same day with one rostral (mouse: 1.33–1.09 anterior/posterior (AP); rat: 2.20–1.60 AP) and one caudal (mouse: 0.97–0.73 AP, rat: 1.20–0.70 AP) brain slice from each animal hemisected so that a total of four slices/data points were collected per animal. All slices were run in parallel, and an additional slice was collected from each animal to serve as a control for slice health and electrode stability throughout the recording period (data available in the repository). The only slices that did not appear stable throughout the experiment had air bubbles that formed under the slice, resulting in the electrodes pushing through the slice; these were excluded. The study was designed to maximize the data collected, allowing for within-subject comparison by measuring DA signals from five different brain regions (dlCPU, vmCPU, core, lshell and mshell) within a single slice. To minimize bias, the first placement within the target region, which had a DA signal exceeding a signal-to-noise (S/N) ratio of 3:1, was used; the researchers did not move the electrode in search of a larger signal within the region. Placements within these regions were marked according to the atlas (Paxinos & Watson, 2013; see Figure S5 for placement records) once a stable baseline was collected. The order in which these measurements were performed was randomized for each slice using randomization.com (seed 3016). The file names were coded so that the researchers were blinded to region and animal during analysis. However, because the male and female cohorts were run and analysed separately, the sex was not blinded during the analysis. Electrode stability was also monitored throughout the course of the experiment by plotting electrode thickness and calibration factors across the placement order to determine if experimental aspects were significantly affecting sensitivity or fouling throughout the course of the experiment. The electrodes proved to be stable throughout the experiment (data available in the repository). No animals were excluded; however, signals from individual brain regions were excluded according to

the following exclusion criteria: if the S/N was less than 3:1, if the placement was later determined to be outside of the region of interest, if a stimulation artifact obscured the true DA peak, or if the release or uptake was statistically determined to be an outlier. One slice was excluded because of a faulty heater not maintaining slice temperature.

## 2.5 | Fast-scan cyclic voltammetry

Carbon fibre microelectrodes (CFMs) were prepared in house using glass capillaries (1.2 mm × .68 mm, A-M Systems, Sequim, WA) and carbon fibres (100–150 µm length, Goodfellow Corp., Berwyn, PA). CFMs were placed in close proximity to a bipolar stimulating electrode (Plastics One, Roanoke, VA) on the surface of the slice. The DA waveform (−0.4 to +1.2 and back to −0.4 V, 400 Vs<sup>−1</sup>, vs. Ag/AgCl) was applied to the electrode and cycled at a frequency of 60 Hz for 5 min followed by 10 Hz for 5 min prior to baseline collections to precondition the electrode and allow it to reach equilibrium. Endogenous DA release was evoked by single electrical pulse stimulation, via a NL800A current stimulus isolator, (monophasic+, 4 ms, 696.1 µA resulting from input of 7.5 V from the Demon Voltammetry software) applied to the tissue every 5 min. Stability was determined after at least 10 collections by looking at the peak height of five consecutive files. If there was no apparent trend towards growth or decline of the signal, the signal was considered stable. The last file collected was analysed and used as the baseline file for that subregion. After reaching this stable baseline, DA signals elicited by single pulse stimulations of sequential increasing intensity (0–756.8 µA, which were the average resulting current intensities resulting from the input of the voltage [V] values shown in Table 1; 60 s interstimulus interval) were collected to generate a stimulus intensity function (later transformed into a stimulus intensity-response curve). This experiment was repeated in the five brain regions within each slice. In a separate control slice, the electrode was placed in the core at the beginning of each experiment, the stimulation was not varied and the placement never changed. All files were collected and analysed with Demon Voltammetry and Analysis software.

Electrodes were calibrated using a multiple linear regression model that used the background current of each electrode to determine its sensitivity (Roberts et al., 2013). A unique set of regression coefficients was generated for the model from over 75 electrodes made within the lab and calibrated using the traditional *in vitro* method of injecting a known concentration of DA (1 µM) using a flow cell apparatus. The background

**TABLE 1** Stimulation inputs and resulting current output.

Input (V)	Output avg (µA)	Output range (µA)
1.4	0.0	0–0
1.6	6.5	0–16
1.8	19.8	8–30
2	38.0	22–50
2.2	58.1	42–70
2.4	79.5	62–93
2.6	100.5	80–116
3	145.7	126–160
3.5	205.1	184–224
4	265.7	242–282
4.5	327.9	301–352
5	389.2	360–408
6	515.2	488–542
7	634.8	608–666
7.5	696.1	672–732
8	756.8	728–797

Note: The stimulus input of 7.5 V was used in baseline recordings, but is not included in the SIR curve inputs.

current at the time of stability was taken to generate a calibration factor for each subregion. In this way, we were able to monitor if electrodes were consistently becoming more or less sensitive throughout the experiment.

Following data collection, NL800A stimulus isolators (Digitimer North America, LLC, Fort Lauderdale, FL) were calibrated following manufacturer recommendations to determine the average stimulating current applied for each intensity step during the stimulus intensity functions. Results are displayed in Table 1.

## 2.6 | Data analysis

### 2.6.1 | Baseline dopamine analysis

A Michaelis–Menten kinetic model was used in the Demon Analysis software to model the DA baseline peak for each brain region.

$$\text{Michaelis–Menten equation: } \frac{d[DA]}{dt} = \frac{f[DA_p] - V_{max}}{\left(\frac{K_m}{[DA]} + 1\right)}. \quad (1)$$

For this analysis, K<sub>m</sub> was left at 160 nM, which is standard for the DAT in the striatum (Wightman

et al., 1988). The monitored output measures included DA release, DA per pulse,  $V_{max}$  and thickness. Thickness is a variable that accounts for the time it takes analytes to diffuse to and away from the electrode surface; it can indirectly approximate fouling of the electrode surface and therefore electrode quality. Uptake was assessed with  $V_{max}$  to provide the most specific information about DAT function. The researcher performing analyses was blinded to the brain region during the analysis and the blinding code was broken only after all data were analysed. The DA release and  $V_{max}$  were each plotted accordingly using GraphPad Prism (v.8.2.1).

## 2.6.2 | Stimulation intensity-response logistic curves

The peak and decay function within Demon Analysis was used to analyse the DA peaks following the stimulation intensity curves. If the DA release was not discernable from the noise the release was not analysed with peak and decay and given a value of zero. Raw DA response data was normalized using logistic transformations for each individual slice. The transformed DA responses were then plotted at each individual, non-continuous applied current from which they were measured. Utilizing the quickpsy package in RStudio Team (RStudio, PBC, Boston, MA), logistic functions were fit to transform individual slice DA response patterns for the 15 applied stimulation currents tested to characterize how increasing these discrete applied currents would change the proportion of DA release. From the fitted logistic function, a 50% Max bisection point and difference threshold (DT; Equation 2) were calculated. These measures were adapted from psychophysics literature where notions of ‘just noticeable differences’ are quantified following Weber’s law (Kingdom, 2016). Here, 50% Max is defined as the stimulation amplitude required to elicit a 50% DA response, or the applied current ( $\mu$ A) where the logistic curve intersects 0.50 (logistically transformed from uM concentrations). The DT is defined as the smallest change in stimulation amplitude that generates a detectable change in DA response. It is calculated with the equation

$$DT = \frac{(ASC(TDR(0.75)) - ASC(TDR(0.25)))}{2}, \quad (2)$$

where ASC is applied stimulation current and TDR is the transformed DA release. Following the individual calculations per slice, generalized linear models from the *glm* package in R were used to fit the mean DA response data with a logistic curve to generate stimulation intensity-response (SIR) curves, using normalized

intervals from 0 to 760  $\mu$ A on the x-axis and the mean transformed DA response to each interval on the y-axis.

## 2.7 | Statistics

### 2.7.1 | Baseline dopamine release and uptake

All statistical analysis for the baseline release and uptake was performed using GraphPad Prism (v8.2.1). Statistical analysis of release and uptake were each done using a two-way ANOVA, where sex and subregion were the two independent variables. First, a Tukey’s multiple comparison post-hoc test was used for differences between subregions in males and females separately. Sidak’s post hoc analysis was used to determine significant sex differences in each of the subregions. Finally, to determine the effects of z-plane, a two-way ANOVA was used, where subregion and z-plane (rostral or caudal) were the two independent variables, followed by Sidak’s post hoc analysis. Generally, Tukey’s multiple comparisons test was used as a first-line statistical test when all possible comparisons were being made, and Sidak’s multiple comparisons test was used for its enhanced statistical power. A linear regression was used to fit the DA release and uptake correlations.

### 2.7.2 | Logistic curves

Mean logistic curves at the group level were calculated based on the mean of all individual curve fits for each slice and then compared between and across groups of sex, z-plane and sub-region using the *glm* function in RStudio. Fifty percent Max and DT values between subregions were compared via mixed effects ANOVA and subsequent post-hoc pairwise *t*-tests to determine significance. For comparisons between sex and z-plane, two-way *t*-tests or one-way ANOVAs were used to determine mean group differences. Significance was based on  $p < 0.05$ .

## 3 | RESULTS

### 3.1 | Baseline dopamine release and uptake

#### 3.1.1 | Mice

DA release was examined in five subregions of male and female mice as presented in Figure 1, with the accompanying statistical analysis in Tables 2 and 3. DA release in

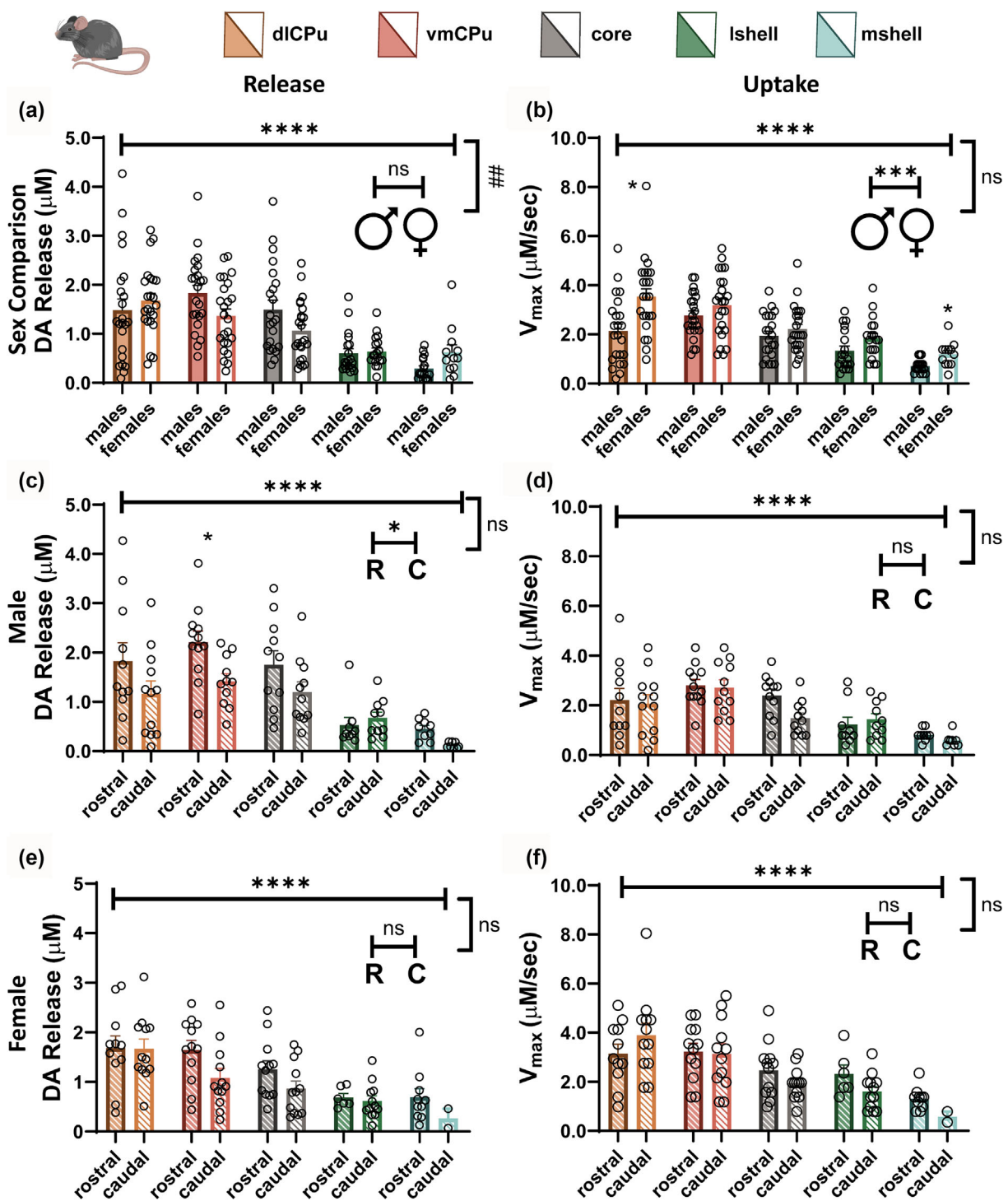


**FIGURE 1** Dopamine (DA) release and uptake in male and female mice. (a) Release collapsed across the z-plane (rostral and caudal) and compared for male and female mice in the five subregions. (b)  $V_{\max}$  collapsed across the z-plane (rostral and caudal) and compared for male and female mice. (c) Release in male mice compared between rostral and caudal signals from the five subregions. (d)  $V_{\max}$  of male mice compared between rostral and caudal signals from the five subregions. (e) Release of female mice compared between rostral and caudal signals from the five subregions. (f)  $V_{\max}$  of female mice compared between rostral and caudal signals from the five subregions. The main effects (\*) and interaction effects (#) are indicated on the graphs with post hoc analysis detailed in Tables 2 and 3. C, caudal; core, nucleus accumbens core; dlCPu, dorsolateral caudate putamen; lshell, nucleus accumbens lateral shell; mshell, nucleus accumbens medial shell; ns, not significant; R, rostral; vmCPu, ventromedial caudate putamen.  $*p < 0.05$ ;  $**p < 0.01$ ;  $***p < 0.001$ ;  $****p < 0.0001$ ;  $\#\#p < 0.01$  interaction effect.

TABLE 2 Posthoc analysis of data presented in Figure 1a,c,e.

<b>Mouse DA release</b>					
<b>Tukey's multiple comparisons test</b>	<b>q</b>	<b>DF</b>	<b>Significant?</b>	<b>Summary</b>	<b>p value</b>
Males	Figure 1a post-hoc analysis				
dlCPu versus vmCPu	1.872	21	No	ns	0.6801
dlCPu versus core	0.04066	21	No	ns	>0.9999
dlCPu versus lshell	5.689	18	Yes	**	0.0063
dlCPu versus mshell	6.422	16	Yes	**	0.0027
vmCPu versus core	2.625	21	No	ns	0.3701
vmCPu versus lshell	8.899	17	Yes	****	<0.0001
vmCPu versus mshell	12.74	16	Yes	****	<0.0001
core versus lshell	6.454	17	Yes	**	0.0022
core versus mshell	8.816	16	Yes	***	0.0001
lshell versus mshell	3.991	13	No	ns	0.0881
Females	Figure 1a post-hoc analysis				
dlCPu versus vmCPu	2.373	22	No	ns	0.4668
dlCPu versus core	6.439	22	Yes	**	0.0013
dlCPu versus lshell	9.916	17	Yes	****	<0.0001
dlCPu versus mshell	6.062	10	Yes	*	0.0108
vmCPu versus core	3.049	23	No	ns	0.2315
vmCPu versus lshell	6.805	17	Yes	**	0.0013
vmCPu versus mshell	4.794	11	Yes	*	0.0387
core versus lshell	6.683	17	Yes	**	0.0016
core versus mshell	3.793	11	No	ns	0.1210
lshell versus mshell	0.1553	6	No	ns	>0.9999
<b>Mouse DA release</b>					
<b>Sidak's multiple comparisons test</b>	<b>t</b>	<b>DF</b>	<b>Significant</b>	<b>Summary</b>	<b>p value</b>
Males versus females	Figure 1a post-hoc analysis				
dlCPu	1.075	195	No	ns	0.8112
vmCPu	2.338	195	No	ns	0.0980
core	2.035	195	No	ns	0.1980
lshell	0.1730	195	No	ns	>0.9999
mshell	1.168	195	No	ns	0.7534
<b>Mouse DA release</b>					
<b>Sidak's multiple comparisons test</b>	<b>t</b>	<b>DF</b>	<b>Significant</b>	<b>Summary</b>	<b>p value</b>
Males	Figure 1C Post-hoc analysis				
Rostral dlCPu versus caudal dlCPu	2.373	39	No	ns	0.1083
Rostral vmCPu versus caudal vmCPu	2.841	39	Yes	*	0.0350
Rostral core versus caudal core	1.999	39	No	ns	0.2366
Rostral lshell versus caudal lshell	0.4853	39	No	ns	0.9931
Rostral mshell versus caudal mshell	0.9677	39	No	ns	0.8739
Females	Figure 1E Post-hoc analysis				
Rostral dlCPu versus caudal dlCPu	0.2140	36	No	ns	0.9999

(Continues)

TABLE 2 (Continued)

<b>Mouse DA release</b>					
<b>Sidak's multiple comparisons test</b>	<b>t</b>	<b>DF</b>	<b>Significant</b>	<b>Summary</b>	<b>p value</b>
Rostral vmCPu versus caudal vmCPu	2.470	36	No	ns	0.0886
Rostral core versus caudal core	1.703	36	No	ns	0.4004
Rostral lshell versus caudal lshell	0.2668	36	No	ns	0.9996
Rostral mshell versus caudal mshell	1.388	36	No	ns	0.6149

Abbreviations: core, nucleus accumbens core; DA, dopamine; dlCPu, dorsolateral caudate putamen; lshell, nucleus accumbens lateral shell; mshell, nucleus accumbens medial shell; vmCPu, ventromedial caudate putamen.

\* $p < 0.05$ .

\*\* $p < 0.01$ .

\*\*\* $p < 0.001$ .

\*\*\*\* $p < 0.0001$ .

TABLE 3 Posthoc analysis of data presented in Figure 1b,d,f.

<b>Mouse DA Vmax</b>					
<b>Tukey's multiple comparisons test</b>	<b>q</b>	<b>DF</b>	<b>Significant?</b>	<b>Summary</b>	<b>Adjusted p value</b>
Males					Figure 1a post-hoc analysis
dlCPu versus vmCPu	2.652	21	No	ns	0.3601
dlCPu versus core	0.8359	21	No	ns	0.9749
dlCPu versus lshell	3.472	18	No	ns	0.1458
dlCPu versus mshell	5.997	16	Yes	**	0.0049
vmCPu versus core	4.496	21	Yes	*	0.0328
vmCPu versus lshell	6.936	17	Yes	**	0.0011
vmCPu versus mshell	11.54	16	Yes	****	<0.0001
core versus lshell	4.047	17	No	ns	0.0708
core versus mshell	8.398	16	Yes	***	0.0002
lshell versus mshell	4.343	13	No	ns	0.0573
Females					Figure 1a post-hoc analysis
dlCPu versus vmCPu	1.563	22	No	ns	0.8019
dlCPu versus core	4.781	22	Yes	*	0.0204
dlCPu versus lshell	6.174	17	Yes	**	0.0034
dlCPu versus mshell	8.702	10	Yes	***	0.0008
vmCPu versus core	4.276	23	Yes	*	0.0433
vmCPu versus lshell	5.463	17	Yes	**	0.0095
vmCPu versus mshell	8.448	11	Yes	***	0.0007
core versus lshell	3.059	17	No	ns	0.2401
core versus mshell	6.379	11	Yes	**	0.0063
lshell versus mshell	6.878	6	Yes	*	0.0158

Mouse DA Vmax

<b>Sidak's multiple comparisons test</b>	<b>t</b>	<b>DF</b>	<b>Significant?</b>	<b>Summary</b>	<b>Adjusted p value</b>
Males versus females					Figure 1b post-hoc analysis
dlCPu	3.273	43.5	Yes	*	0.0104
vmCPu	1.310	41.77	No	ns	0.6670

TABLE 3 (Continued)

<b>Mouse DA Vmax</b>					
<b>Sidak's multiple comparisons test</b>	<b>t</b>	<b>DF</b>	<b>Significant?</b>	<b>Summary</b>	<b>Adjusted p value</b>
core	0.9969	43.94	No	ns	0.8591
lshell	1.877	34.61	No	ns	0.3002
mshell	3.005	15.31	Yes	*	0.0429

<b>Mouse DA Vmax</b>					
<b>Sidak's multiple comparisons test</b>	<b>t</b>	<b>DF</b>	<b>Significant?</b>	<b>Summary</b>	<b>Adjusted p value</b>
Males	Figure 1d post-hoc analysis				
Rostral dlCPu versus caudal dlCPu	0.3799	39	No	ns	0.9978
Rostral vmCPu versus caudal vmCPu	0.2210	39	No	ns	0.9998
Rostral core versus caudal core	2.303	39	No	ns	0.1267
Rostral lshell versus caudal lshell	0.4791	39	No	ns	0.9935
Rostral mshell versus caudal mshell	0.4614	39	No	ns	0.9945
Females	Figure 1f post-hoc analysis				
Rostral dlCPu versus caudal dlCPu	1.882	36	No	ns	0.2965
Rostral vmCPu versus caudal vmCPu	0.2208	36	No	ns	0.9998
Rostral core versus caudal core	1.291	36	No	ns	0.6824
Rostral lshell versus caudal lshell	1.269	36	No	ns	0.6976
Rostral mshell versus caudal mshell	1.398	36	No	ns	0.6076

Abbreviations: core, nucleus accumbens core; DA, dopamine; dlCPu, dorsolateral caudate putamen; lshell, nucleus accumbens lateral shell; mshell, nucleus accumbens medial shell; vmCPu, ventromedial caudate putamen.

\* $p < 0.05$ .

\*\* $p < 0.01$ .

\*\*\* $p < 0.001$ .

\*\*\*\* $p < 0.0001$ .

male and female mice was significantly different across the five subregions examined ( $F(4,149) = 29.29$ ;  $p < 0.0001$ ), and though no overall effect of sex was found ( $F(1,46) = 0.2564$ ;  $p = 0.6150$ ), there was a significant interaction effect between the two ( $F(4,149) = 3.517$ ;  $p = 0.0089$ ) as determined via a two-way ANOVA (Figure 1a). Post-hoc analysis using Tukey's multiple comparison test showed significant differences in release between the subregions, as highlighted in Table 2. Additionally, Sidak's multiple comparison post-hoc analysis did not find any sex differences in any of the subregions (Figure 1a, Table 2). Release was further broken down across the z-plane into rostral and caudal subregions and analysed using a two-way ANOVA followed by a Sidak's multiple comparison post-hoc analysis. The male mice displayed a significant main effect of subregions ( $F(4,44) = 15.84$ ,  $p < 0.0001$ ) and z-plane ( $F(1,11) = 9.343$ ,  $p = 0.0109$ ) with no significant interaction effect ( $F(4,28) = 1.617$ ,  $p = 0.1977$ ) and post-hoc analysis found the vmCPu showed a significant difference across the z-plane (Figure 1c, Table 2). The female mice displayed a significant main effect of subregions ( $F(4,44) = 15.32$ ,

$p < 0.0001$ ) but not z-plane ( $F(1,11) = 4.405$ ,  $p = 0.0597$ ) and no significant interaction effect ( $F(4,25) = 1.617$ ,  $p = 0.3633$ ).

The DA uptake, assessed as  $V_{max}$ , from the five subregions of male and female mice was determined and is presented in Figure 1 with the accompanying statistical analysis in Table 3. The uptake in male and female mice was evaluated using a two-way ANOVA, which found a significant main effect of the five subregions examined ( $F(2.714,101.1) = 26.41$ ;  $p < 0.0001$ ), along with a main effect of sex ( $F(1,46) = 13.05$ ;  $p = 0.0007$ ), but lacking a significant interaction effect ( $F(4,149) = 2.339$ ;  $p = 0.596$ ) (Figure 1b). Post-hoc analysis using a Tukey's multiple comparison test showed significant differences in  $V_{max}$  between the subregions in male and female mice, as highlighted in Table 3. Additionally, Sidak's multiple comparison post-hoc analysis found sex differences only in the dlCPu and mshell subregions (Figure 1b, Table 3). The uptake of each subregion was divided into rostral and caudal z-planes, and a two-way ANOVA followed by a Sidak's multiple comparison post-hoc analysis was used to determine if there were any differences across the

z-plane. The male mice displayed a significant main effect of subregions ( $F(4,44) = 14.32, p < 0.0001$ ) but not z-plane ( $F(1,11) = 1.561, p = 0.2375$ ) and no significant interaction effect ( $F(4,28) = 1.047, p = 0.4006$ ). The female mice displayed a significant main effect of subregions ( $F(4,44) = 11.67, p < 0.0001$ ) but not z-plane ( $F(1,11) = 1.1985, p = 0.2971$ ) and no significant interaction effect ( $F(4,25) = 2.515, p = 0.0669$ ).

The results in mice show that DA release and uptake were generally higher in dorsal regions, as compared with most ventral regions (lshell and mshell), and females exhibited faster DA uptake than males.

### 3.1.2 | Rats

The same experiments were conducted simultaneously in rats. DA release was examined in five subregions of male and female rats and presented in Figure 2, with the accompanying statistical analysis in Table 4. DA release in rats was analysed using a two-way ANOVA, which revealed significant main effects of subregion ( $F(2.628,97.88) = 25.01, p < 0.0001$ ) and sex ( $F(1,43) = 9.579, p = 0.0033$ ), with no interaction effect ( $F(4,149) = 2.266, p = 0.0677$ ) (Figure 2a). Post-hoc analysis of subregion differences was determined using a Tukey's multiple comparison test, and the results are detailed in Table 4. A Sidak's multiple comparison test was used as a separate post-hoc analysis and found that of the subregions evaluated, only the core had a significantly different release between males and females (Figure 2a, Table 4). DA release was then further subdivided into rostral and caudal to determine the effect of the z-plane and a two-way ANOVA followed by a Sidak's multiple comparison post-hoc analysis was performed. The male rats displayed a significant main effect of subregions ( $F(4,44) = 15.38, p < 0.0001$ ) but not z-plane ( $F(1,11) = 0.2959, p = 0.5973$ ) with a significant interaction effect ( $F(4,32) = 6.138, p = 0.0009$ ) and post-hoc analysis found the vmCPu and the core showed a significant difference across the z-plane (Figure 2c, Table 4). The female rats displayed a significant main effect of subregions ( $F(4,44) = 13.93, p < 0.0001$ ) but not z-plane ( $F(1,11) = 1.370, p = 0.2666$ ) and no significant interaction effect ( $F(4,18) = 2.247, p = 0.1044$ ).

The DA uptake, or  $V_{max}$ , from the five subregions of male and female rats was determined and is presented in Figure 2, with the accompanying statistical analysis in Table 5. DA uptake was analysed using a two-way ANOVA, which revealed a significant main effect of subregion ( $F(3.299,122.9) = 2704, p < 0.0001$ ), but not

sex ( $F(1,43) = 0.4462, p = 0.6852$ ), and no interaction effect ( $F(4,149) = 2.410, p = 0.0969$ ) (Figure 2b).  $V_{max}$  was divided by the z-plane into rostral and caudal, and a two-way ANOVA followed by a Sidak's multiple comparison test was used. The male rats displayed a significant main effect of subregions ( $F(4,44) = 15.29, p < 0.0001$ ) but not z-plane ( $F(1,11) = 1.143, p = 0.3079$ ) or significant interaction effect ( $F(4,32) = 2.065, p = 0.1087$ ). The female rats displayed a significant main effect of subregions ( $F(4,44) = 14.71, p < 0.0001$ ) but not z-plane ( $F(1,11) = 1.250, p = 0.2874$ ) and no significant interaction effect ( $F(4,18) = 1.252, p = 0.3250$ ).

The highest DA release in rats was observed in the vmCPu and NAc core, and there was a lack of a strong dorsal-to-ventral gradient in DA uptake. In contrast to what was observed in mice, DA uptake did not tend to be different between sexes, while DA release tended to be lower in females than males.

While the purpose of this study was not to compare between species, it is apparent from the data that mice and rats generally differed in DA measures, with lower release and slower reuptake in the rats.

## 3.2 | Release and uptake correlations

The release and uptake of DA often demonstrate a correlation with one another as uptake increases along with increasing release. To determine if release and uptake were significantly correlated, a linear regression was calculated and if the line was significantly non-zero, the relationship was considered significantly correlated (Figure 3, Table 6). The only regions that did not display a significant correlation between release and uptake were the mouse male mshell and the rat female dlCPu (Figure 3, Table 6). The relationship between release and uptake can also be evaluated as a ratio of the two measures. The release-to-uptake ratio was calculated for each subregion and initially compared by sex (Table 6). Sex differences were found in all the subregions of both mice and rats, with the sole exception of the mshell of mice. The subregions were then collapsed across sexes and compared using a one-way ANOVA followed by a Tukey's post hoc test. Significant main effects of subregion were found in both mice ( $F(2.689,102.9) = 7.680, p = 0.0002$ ) and rats ( $F(3.219,123.1) = 16.72, p < 0.0001$ ), with all post hoc analysis results displayed in Table 6.

From these calculations, we observed that the ratio of release to uptake was higher in mice than rats and higher in males than females in both species.

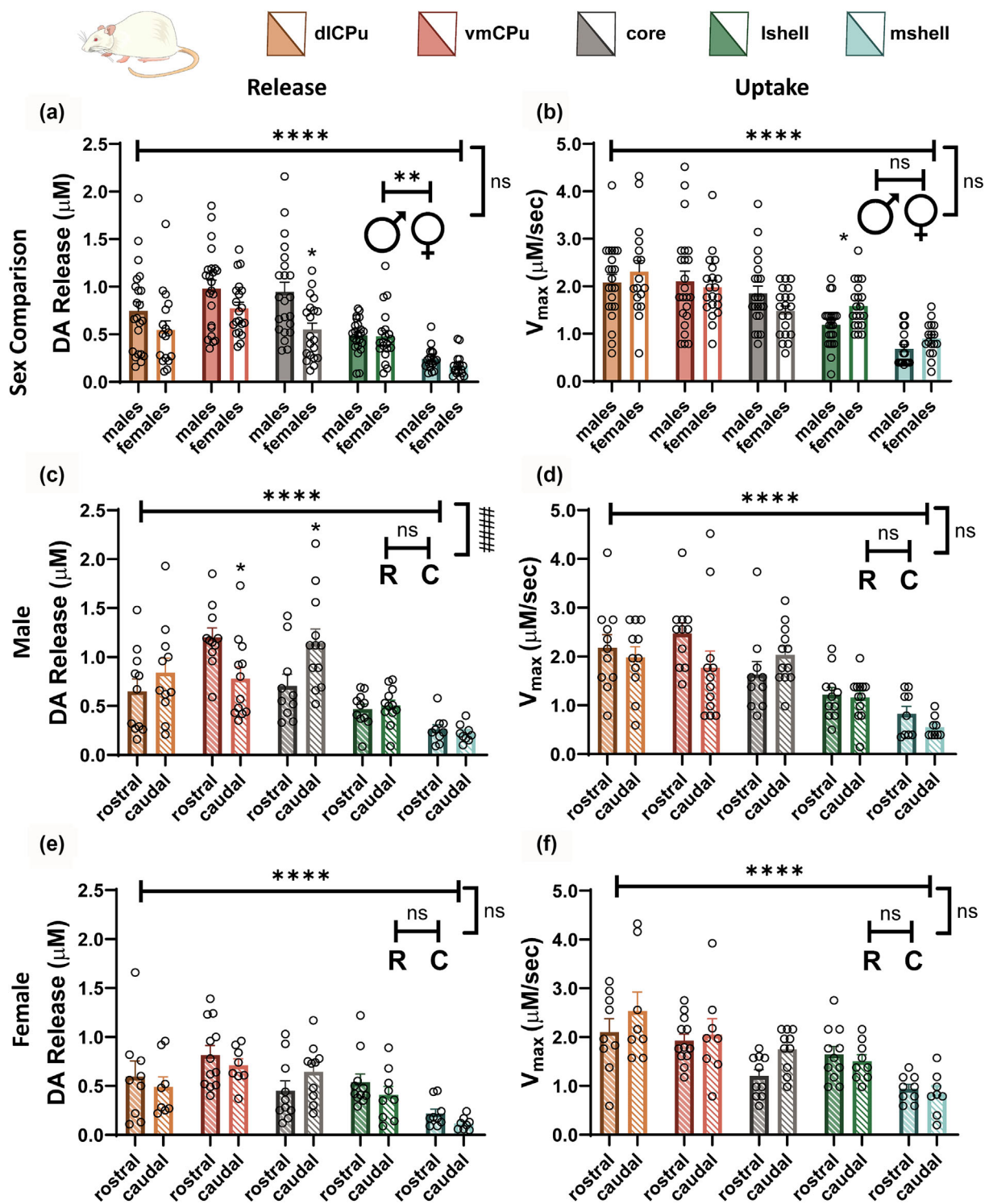


**FIGURE 2** Dopamine (DA) release and uptake in male and female rats. (a) Release collapsed across the z-plane (rostral and caudal) and compared for male and female rats in the five subregions. (b)  $V_{\max}$  collapsed across z-plane (rostral and caudal) and compared for male and female rats. (c) Release of male rats compared between rostral and caudal signals from the five subregions. (d)  $V_{\max}$  of male rats compared between rostral and caudal signals from the five subregions. (e) Release of female rats compared between rostral and caudal signals from the five subregions. (f)  $V_{\max}$  of female rats compared between rostral and caudal signals from the five subregions. The main effects (\*) and interaction effects (#) are indicated on the graphs with post hoc analysis detailed in Tables 4 and 5. C, caudal; core, nucleus accumbens core; dlCPu, dorsolateral caudate putamen; Ishell, nucleus accumbens lateral shell; mshell, nucleus accumbens medial shell; ns, not significant; R, rostral; vmCPu, ventromedial caudate putamen. \* $p < 0.05$ ; \*\* $p < 0.01$ ; \*\*\* $p < 0.001$ ; \*\*\*\* $p < 0.0001$ ; ##### $p < 0.0001$  interaction effect.

TABLE 4 Posthoc analysis of data presented in Figure 2a,c,e.

<b>Rat DA release</b>					
<b>Tukey's multiple comparisons test</b>	<b>q</b>	<b>DF</b>	<b>Significant?</b>	<b>Summary</b>	<b>p value</b>
Males	Figure 2a post-hoc analysis				
dlCPu versus vmCPu	2.21	21	No	ns	0.5359
dlCPu versus core	2.56	20	No	ns	0.3954
dlCPu versus lshell	3.373	21	No	ns	0.1585
dlCPu versus mshell	9.127	16	Yes	****	<0.0001
vmCPu versus core	0.3627	21	No	ns	0.9990
vmCPu versus lshell	8.142	22	Yes	****	<0.0001
vmCPu versus mshell	12.12	17	Yes	****	<0.0001
core versus lshell	6.015	21	Yes	**	0.0029
core versus mshell	9.125	17	Yes	****	<0.0001
lshell versus mshell	8.134	17	Yes	***	0.0002
Females	Figure 2a post-hoc analysis				
dlCPu versus vmCPu	3.176	14	No	ns	0.2196
dlCPu versus core	0.0529	15	No	ns	>0.9999
dlCPu versus lshell	0.8763	14	No	ns	0.9695
dlCPu versus mshell	5.775	14	Yes	**	0.0083
vmCPu versus core	4.369	17	Yes	*	0.0456
vmCPu versus lshell	5.977	17	Yes	**	0.0045
vmCPu versus mshell	14.53	15	Yes	****	<0.0001
Core versus lshell	1.229	17	No	ns	0.9042
Core versus mshell	7.792	15	Yes	***	0.0005
Lshell versus mshell	7.608	14	Yes	***	0.0008
<b>Rat DA release</b>					
<b>Sidak's multiple comparisons test</b>	<b>t</b>	<b>DF</b>	<b>Significant?</b>	<b>Summary</b>	<b>p value</b>
Males versus females	Figure 2a post-hoc analysis				
dlCPu	1.457	36.51	No	ns	0.5654
vmCPu	1.904	38.95	No	ns	0.2830
core	3.167	36.29	Yes	*	0.0155
lshell	0.1033	32.00	No	ns	>0.9999
mshell	1.75	32.9	No	ns	0.3742
<b>Rat DA release</b>					
<b>Sidak's multiple comparisons test</b>	<b>t</b>	<b>DF</b>	<b>Significant?</b>	<b>Summary</b>	<b>p value</b>
Males	Figure 2c post-hoc analysis				
Rostral dlCPu versus caudal dlCPu	1.377	43	No	ns	0.6194
Rostral vmCPu versus caudal vmCPu	3.060	43	Yes	*	0.0189
Rostral core versus caudal core	3.239	43	Yes	*	0.0115
Rostral lshell versus caudal lshell	0.2757	43	No	ns	0.9995
Rostral mshell versus caudal mshell	0.3685	43	No	ns	0.9981
Females	Figure 2e post-hoc analysis				
Rostral dlCPu versus caudal dlCPu	1.457	29	No	ns	0.5710
Rostral vmCPu versus caudal vmCPu	0.8110	29	No	ns	0.9366

TABLE 4 (Continued)

<b>Rat DA release</b>					
<b>Sidak's multiple comparisons test</b>	<b>t</b>	<b>DF</b>	<b>Significant?</b>	<b>Summary</b>	<b>p value</b>
Rostral core versus caudal core	1.845	29	No	ns	0.3240
Rostral lshell versus caudal lshell	1.462	29	No	ns	0.5679
Rostral mshell versus caudal mshell	1.111	29	No	ns	0.8007

Abbreviations: core, nucleus accumbens core; DA, dopamine; dlCPu, dorsolateral caudate putamen; lshell, nucleus accumbens lateral shell; mshell, nucleus accumbens medial shell; vmCPu, ventromedial caudate putamen.

\* $p < 0.05$ .

\*\* $p < 0.01$ .

\*\*\* $p < 0.001$ .

\*\*\*\* $p < 0.0001$ .

TABLE 5 Posthoc analysis of data presented in Figure 2b,d,f.

<b>Rat DA Vmax</b>					
<b>Tukey's multiple comparisons test</b>	<b>q</b>	<b>DF</b>	<b>Significant?</b>	<b>Summary</b>	<b>Adjusted p value</b>
Males	Figure 1b post-hoc analysis				
dlCPu versus vmCPu	0.1221	21	No	ns	>0.9999
dlCPu versus core	1.324	20	No	ns	0.8794
dlCPu versus lshell	6.750	21	Yes	***	0.0009
dlCPu versus mshell	11.16	16	Yes	****	<0.0001
vmCPu versus core	1.373	21	No	ns	0.8652
vmCPu versus lshell	6.022	22	Yes	**	0.0027
vmCPu versus mshell	8.468	17	Yes	***	0.0001
core versus lshell	4.383	21	Yes	*	0.0389
core versus mshell	8.729	17	Yes	****	<0.0001
lshell versus mshell	6.919	17	Yes	**	0.0011
Females	Figure 1b post-hoc analysis				
dlCPu versus vmCPu	2.22	14	No	ns	0.5383
dlCPu versus core	5.087	15	Yes	*	0.019
dlCPu versus lshell	4.01	14	No	ns	0.0825
dlCPu versus mshell	9.303	14	Yes	***	0.0001
vmCPu versus core	3.624	17	No	ns	0.1227
vmCPu versus lshell	3.122	17	No	ns	0.2238
vmCPu versus mshell	10.86	15	Yes	****	<0.0001
core versus lshell	1.056	17	No	ns	0.9421
core versus mshell	5.247	15	Yes	*	0.0153
lshell versus mshell	7.887	14	Yes	***	0.0006

<b>Rat DA Vmax</b>					
<b>Sidak's multiple comparisons test</b>	<b>t</b>	<b>DF</b>	<b>Significant?</b>	<b>Summary</b>	<b>Adjusted p value</b>
Males versus females	Figure 1b post-hoc analysis				
dlCPu	0.7757	30.97	No	ns	0.9468
vmCPu	0.4863	38.17	No	ns	0.9930
core	1.942	37.20	No	ns	0.2650

(Continues)

TABLE 5 (Continued)

<b>Rat DA Vmax</b>					
<b>Sidak's multiple comparisons test</b>	<b>t</b>	<b>DF</b>	<b>Significant?</b>	<b>Summary</b>	<b>Adjusted p value</b>
lshell	2.750	39.78	Yes	*	0.0438
mshell	1.701	33.00	No	ns	0.4040
<b>Rat DA Vmax</b>					
<b>Sidak's multiple comparisons test</b>	<b>t</b>	<b>DF</b>	<b>Significant?</b>	<b>Summary</b>	<b>Adjusted p value</b>
Males	Figure 1d post-hoc analysis				
Rostral dlCPu versus caudal dlCPu	0.6237	43	No	ns	0.9785
Rostral vmCPu versus caudal vmCPu	2.413	43	No	ns	0.0969
Rostral core versus caudal core	1.403	43	No	ns	0.6010
Rostral lshell versus caudal lshell	0.1987	43	No	ns	<0.9999
Rostral mshell versus caudal mshell	0.9239	43	No	ns	0.8932
Females	Figure 1f post-hoc analysis				
Rostral dlCPu versus caudal dlCPu	1.368	29	No	ns	0.6336
Rostral vmCPu versus caudal vmCPu	0.3907	29	No	ns	0.9975
Rostral core versus caudal core	1.980	29	No	ns	0.2554
Rostral lshell versus caudal lshell	0.5315	29	No	ns	0.9896
Rostral mshell versus caudal mshell	0.2302	29	No	ns	0.9998

Abbreviations: core, nucleus accumbens core; DA, dopamine; dlCPu, dorsolateral caudate putamen; lshell, nucleus accumbens lateral shell; mshell, nucleus accumbens medial shell; vmCPu, ventromedial caudate putamen.

\* $p < 0.05$ .

\*\* $p < 0.01$ .

\*\*\* $p < 0.001$ .

\*\*\*\* $p < 0.0001$ .

### 3.3 | Stimulation intensity-response (SIR) curves

#### 3.3.1 | Mice

We evaluated how DA release responded to varying applied stimulation currents utilizing a logistic transformation of the DA response data and then fitting the response data with a logistic curve to generate stimulation intensity-response (SIR) curves (Figures 4–7). The curve was fit to the transformed DA release at each applied current first for each individual slice, then averaged across specific groups of interest (i.e., z-plane, sex, subregion). To evaluate different portions of this curve, the 50% Max and DT were calculated based on each curve. Male mice showed significant differences in 50% Max when comparing between subregions (Figure 4a;  $F(4,99) = 5.974$ ,  $p = 0.0002$ ), and a post-hoc pairwise *t*-test found the following significant differences between subregions: dlCPu versus vmCPu ( $p = 0.0009$ ); vmCPu versus core ( $p = 0.0026$ ); vmCPu versus lshell ( $p = 8.9e-06$ ); vmCPu versus mshell ( $p = 0.0007$ ). The curves were further broken down by z-plane (rostral or caudal). The

male rostral curves demonstrated a significant effect of subregion on 50% Max (Figure 4c;  $F(4,47) = 5.046$ ,  $p = 0.0018$ ), with the following differences between subregions as determined by a pair-wise post-hoc *t*-test: vmCPu versus dlCPu ( $p = 0.0056$ ); vmCPu versus core ( $p = 0.0190$ ); vmCPu versus lshell ( $p = 0.0002$ ); vmCPu versus mshell ( $p = 0.0499$ ). Likewise, the male caudal curves also had significant differences in 50% Max between the subregions (Figure 4e;  $F(4,47) = 3.586$ ,  $p = 0.0124$ ), with a post-hoc pairwise *t*-test revealing the following individual differences: vmCPu versus dlCPu ( $p = 0.037$ ); vmCPu versus core ( $p = 0.016$ ); vmCPu versus lshell ( $p = 0.0079$ ); vmCPu versus mshell ( $p = 0.0012$ ). No significant differences were observed in DT in male mice when comparing between subregions or when broken down by the z-plane (Figure 4a,c,e). Female mice did not demonstrate differences in 50% Max or DT when comparing between subregions or when broken down by z-plane (Figure 4b,d,f). Each subregion was also broken down within sex into rostral and caudal curves to determine if the z-plane significantly affected 50% Max or DT (Figure S1). The only regions that displayed an effect of the z-plane were the mshell in males, with a

**FIGURE 3** Dopamine (DA) release and uptake correlations in male and female mice and rats. (a) DA release and uptake correlations for mice in the dorsolateral caudate putamen (dlCPu) (a), ventromedial caudate putamen (vmCPu) (c), nucleus accumbens core (core) (e), nucleus accumbens lateral shell (lshell) (g) and nucleus accumbens medial shell (mshell) (i). DA release and uptake correlations for rats in the dlCPu (b), vmCPu (d), core (f), lshell (h) and mshell (j). The sexes were collapsed to compare the five subregions in mice (k) and rats (l). The stars next to each legend indicate if the line is significantly non-zero, additional statistical analysis and comparisons are detailed in Table 6. \* $p < 0.05$ ; \*\* $p < 0.01$ ; \*\*\* $p < 0.001$ ; \*\*\*\* $p < 0.0001$ .

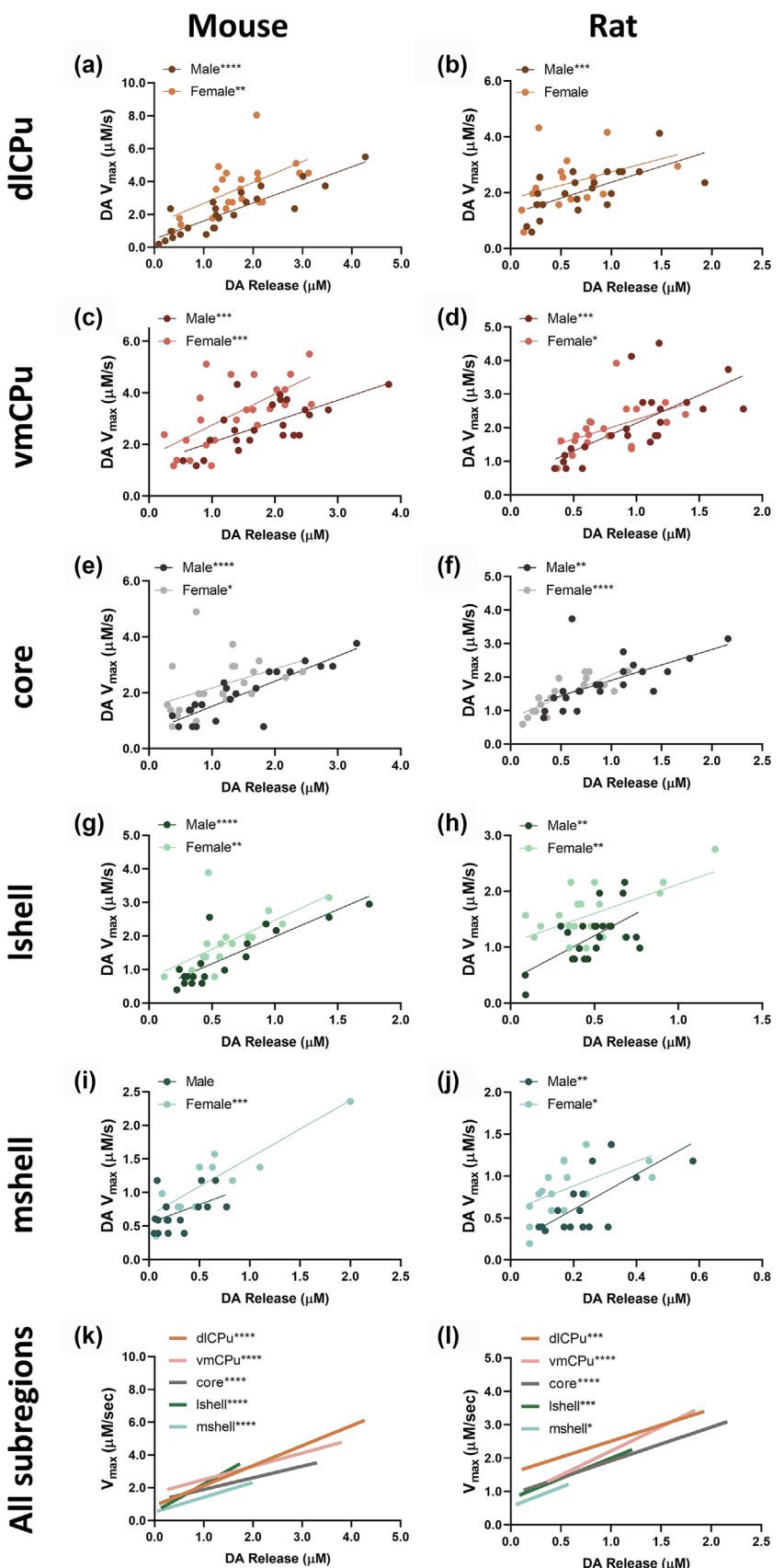


TABLE 6 Statistical analysis of data presented in Figure 3.

Sex difference comparison						
Sex	Subregion	Release/uptake $\pm$ SEM	Slope	R2	Significantly non-zero?	Difference in ratios?
Mouse						
Male	dICPu	0.6964 $\pm$ 0.0556	1.098 $\pm$ 0.1308	0.7702	F(1,21) = 70.40, $p < 0.0001$	$p = 0.0035$
Female	dICPu	0.4923 $\pm$ 0.0330	1.271 $\pm$ 0.3706	0.3589	F(1,21) = 11.76, $p = 0.0025$	
Male	vmCPu	0.6693 $\pm$ 0.0387	0.8135 $\pm$ 0.1961	0.4504	F(1,21) = 17.21, $p = 0.0005$	$p < 0.0001$
Female	vmCPu	0.4371 $\pm$ 0.0346	1.199 $\pm$ 0.2896	0.438	F(1,22) = 17.15, $p = 0.0004$	
Male	core	0.7819 $\pm$ 0.0826	0.9000 $\pm$ 0.1202	0.7369	F(1,20) = 56.02, $p < 0.0001$	$p = 0.0033$
Female	core	0.4936 $\pm$ 0.0425	0.6826 $\pm$ 0.3067	0.1838	F(1,22) = 4.954, $p = 0.0366$	
Male	lshell	0.4641 $\pm$ 0.0301	1.613 $\pm$ 0.2439	0.7202	F(1,17) = 43.77, $p < 0.0001$	$p = 0.0181$
Female	lshell	0.3603 $\pm$ 0.0272	1.729 $\pm$ 0.5195	0.4092	F(1,16) = 11.08, $p = 0.0043$	
Male	mshell	0.4104 $\pm$ 0.0654	0.5467 $\pm$ 0.2677	0.2176	F(1,15) = 4.171, $p = 0.0591$	$p = 0.5491$
Female	mshell	0.4693 $\pm$ 0.0617	0.8566 $\pm$ 0.1530	0.7581	F(1,10) = 31.33, $p = 0.0002$	
Rat						
Male	dICPu	0.3518 $\pm$ 0.0340	1.143 $\pm$ 0.2945	0.4297	F(1,20) = 15.07, $p = 0.0009$	$p = 0.0430$
Female	dICPu	0.2404 $\pm$ 0.0337	0.9505 $\pm$ 0.5776	0.1529	F(1,15) = 2.707, $p = 0.1207$	
Male	vmCPu	0.4932 $\pm$ 0.0282	1.662 $\pm$ 0.3900	0.4639	F(1,21) = 18.17, $p = 0.0003$	$p = 0.0320$
Female	vmCPu	0.4059 $\pm$ 0.0293	1.172 $\pm$ 0.4738	0.2537	F(1,18) = 6.118, $p = 0.0236$	
Male	core	0.5130 $\pm$ 0.0346	0.9210 $\pm$ 0.2684	0.3706	F(1,20) = 11.78, $p = 0.0026$	$p = 0.0013$
Female	core	0.3513 $\pm$ 0.0287	1.300 $\pm$ 0.2167	0.6666	F(1,18) = 35.99, $p < 0.0001$	
Male	lshell	0.4350 $\pm$ 0.0303	1.593 $\pm$ 0.4465	0.3775	F(1,21) = 12.73, $p = 0.0018$	$p = 0.0058$
Female	lshell	0.3062 $\pm$ 0.0306	1.043 $\pm$ 0.3326	0.3535	F(1,18) = 9.840, $p = 0.0057$	
Male	mshell	0.3872 $\pm$ 0.0378	2.092 $\pm$ 0.5882	0.4415	F(1,16) = 12.65, $p = 0.0026$	$p = 0.0004$
Female	mshell	0.2011 $\pm$ 0.0258	1.466 $\pm$ 0.5536	0.3185	F(1,15) = 7.009, $p = 0.0183$	
Subregion comparison						
Subregion	Release/uptake $\pm$ SEM		Slope	R2	Significantly non-zero?	Difference in ratio?
Mouse						
dICPu	0.5943 $\pm$ 0.0365		1.219 $\pm$ 0.1861	0.4936	F(1,44) = 42.89, $p < 0.0001$	dICPu versus vmCPu $p = 0.7068$
vmCPu	0.5507 $\pm$ 0.0314		0.8134 $\pm$ 0.1841	0.3026	F(1,45) = 19.53, $p < 0.0001$	dICPu versus core $p = 0.9713$
core	0.6315 $\pm$ 0.0511		0.7095 $\pm$ 0.1508	0.3348	F(1,44) = 22.15, $p < 0.0001$	dICPu versus lshell $p = 0.0011$
lshell	0.4136 $\pm$ 0.0220		1.684 $\pm$ 0.2680	0.5301	F(1,35) = 39.45, $p < 0.0001$	dICPu versus mshell $p = 0.0332$
mshell	0.4348 $\pm$ 0.0480		0.9021 $\pm$ 0.1258	0.6558	F(1,27) = 51.45, $p < 0.0001$	vmCPu versus core $p = 0.5763$
						vmCPu versus lshell $p = 0.0033$
						vmCPu versus mshell $p = 0.0836$
						core versus lshell $p = 0.0008$
						core versus mshell $p = 0.085$
						$p = 0.9906$

TABLE 6 (Continued)

Subregion comparison						
Subregion	Release/uptake ± SEM	Slope	R2	Significantly non-zero?	Comparison	Difference in ratio?
Rat					lshell versus mshell	
dlCPu	0.3033 ± 0.0257	0.9586 ± 0.2852	0.2339	F(1,37) = 11.30, p = 0.0018	dlCPu versus vmCPu	p < 0.0001
vmCPu	0.4526 ± 0.0214	1.451 ± 0.2826	0.3914	F(1,41) = 26.37, p < 0.0001	dlCPu versus core	p < 0.0001
core	0.4360 ± 0.0254	1.009 ± 0.1623	0.4917	F(1,40) = 38.69, p < 0.0001	dlCPu versus lshell	p = 0.0341
lshell	0.3751 ± 0.0243	1.211 ± 0.2971	0.2884	F(1,41) = 16.52, p = 0.0002	dlCPu versus mshell	p = 0.9996
mshell	0.2968 ± 0.0280	1.161 ± 0.4900	0.1454	F(1,33) = 5.615, p = 0.0238	vmCPu versus core	p = 0.9232
					vmCPu versus lshell	p = 0.0042
					vmCPu versus mshell	p = 0.0002
					core versus lshell	p = 0.0574
					core versus mshell	p < 0.0001
					lshell versus mshell	p = 0.0515

Abbreviations: core, nucleus accumbens core; dlCPu, dorsolateral caudate putamen; lshell, nucleus accumbens lateral shell; mshell, nucleus accumbens medial shell; vmCPu, ventromedial caudate putamen.

significant difference in 50% Max ( $F(1,15) = 9.212$ ,  $p = 0.0083$ ; Figure S1I), and the lshell in females, which had a significant difference in 50% Max ( $F(1,16) = 9.562$ ,  $p = 0.0070$ ; Figure S1H).

The SIR curves were further compared by sex in Figure 5. All subregions were combined to provide an overall sex comparison (Figure 5a); however, no differences were found in either 50% Max or DT. The individual subregions were also compared by sex and no differences were observed in either 50% Max or DT (Figure 5b–f). Additionally, curves from individual subregions were also broken down by z-plane and compared, with no sex differences found in either rostral or caudal curves (Figure S2).

A noteworthy finding in the mouse SIR curve analysis is that a subregion difference, namely, a lower 50% Max in the vmCPu compared with every other subregion, was apparent only in the males of the species. This is apparent even though differences were not found when comparing males and females across each subregion.

### 3.3.2 | Rats

Male rats showed significant differences in 50% Max when comparing between subregions (Figure 6a;  $F(4,103) = 2.52$ ,  $p = 0.0457$ ), and a post-hoc pairwise *t*-test found a significant difference between the vmCPu and the mshell ( $p = 0.0272$ ). In contrast, female rats showed a significant difference in DT between subregions ( $F(4,89) = 3.466$ ,  $p = 0.0112$ ) (Figure 6b). A post-hoc pairwise *t*-test found the following significant differences between subregions: vmCPu versus lshell ( $p = 0.0032$ ); vmCPu versus mshell ( $p = 0.0035$ ). The male and female curves were each further broken down by z-plane. Male rostral curves demonstrated a significant effect of subregion on DT (Figure 6c;  $F(4,47) = 3.075$ ,  $p = 0.0249$ ) with the following differences between subregions as determined by a pair-wise post-hoc *t*-test: vmCPu versus mshell ( $p = 0.031$ ); lshell versus mshell ( $p = 0.012$ ). No significant differences were observed in either 50% Max or DT in male caudal curves (Figure 6e) or female rostral

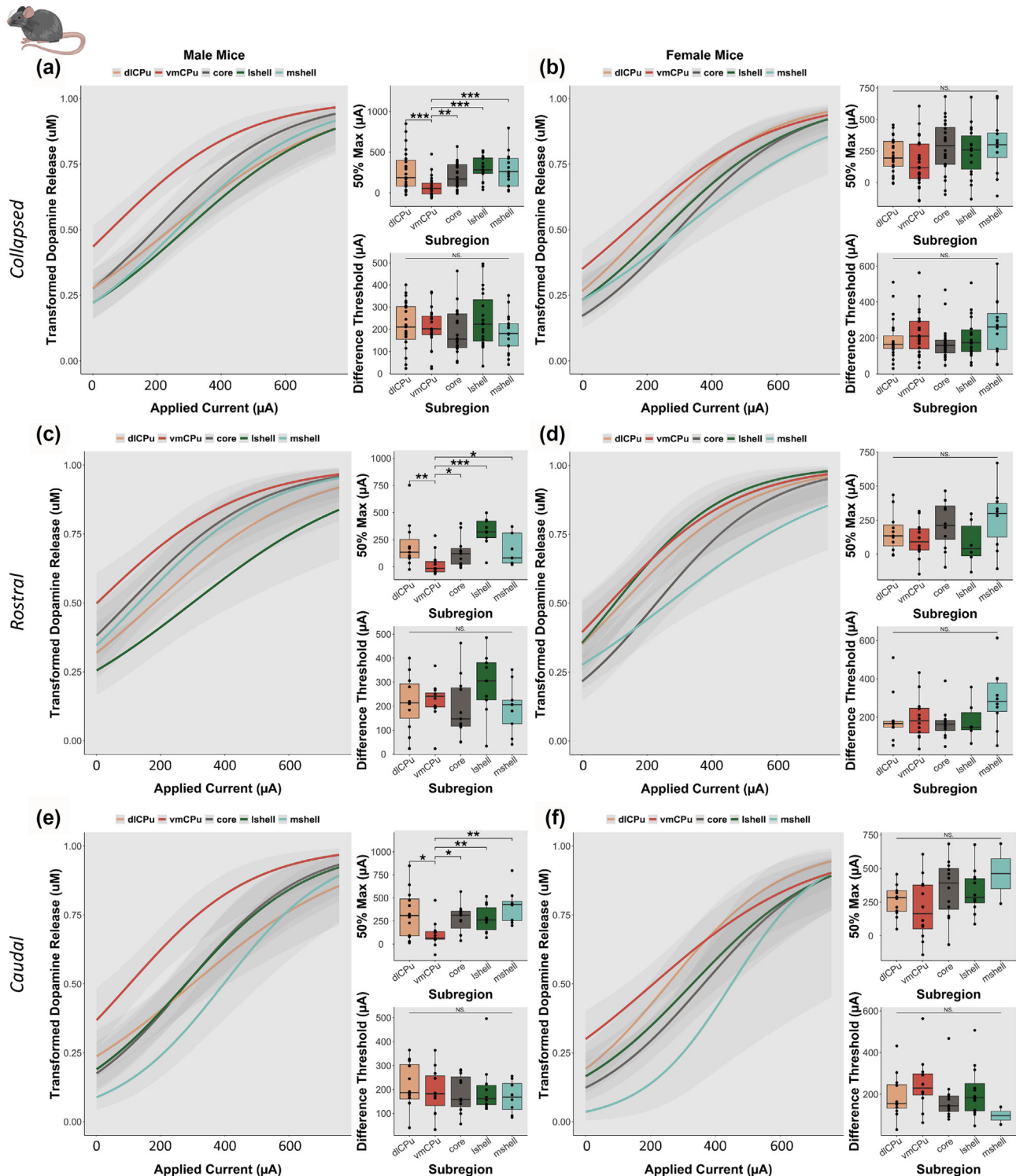


**FIGURE 4** Stimulus intensity response curves comparing transformed dopamine (DA) release of mice for each applied current between subregions. (a) Stimulus intensity response curve by subregion for male mice collapsed across z-plane (rostral and caudal) with 50% Max calculation and difference threshold for each subregion based on stimulus intensity response curve for male mice collapsed across z-plane. (b) For female mice collapsed across z-plane. (c) For male mice rostral z-plane only. (d) For female mice rostral z-plane only. (e) For male mice caudal z-plane only. (f) For female mice caudal z-plane only. core, nucleus accumbens core; dlCPu, dorsolateral caudate putamen; lshell, nucleus accumbens lateral shell; mshell, nucleus accumbens medial shell; vmCPu, ventromedial caudate putamen. \* $p < 0.05$ ; \*\* $p < 0.01$ ; \*\*\* $p < 0.001$ .

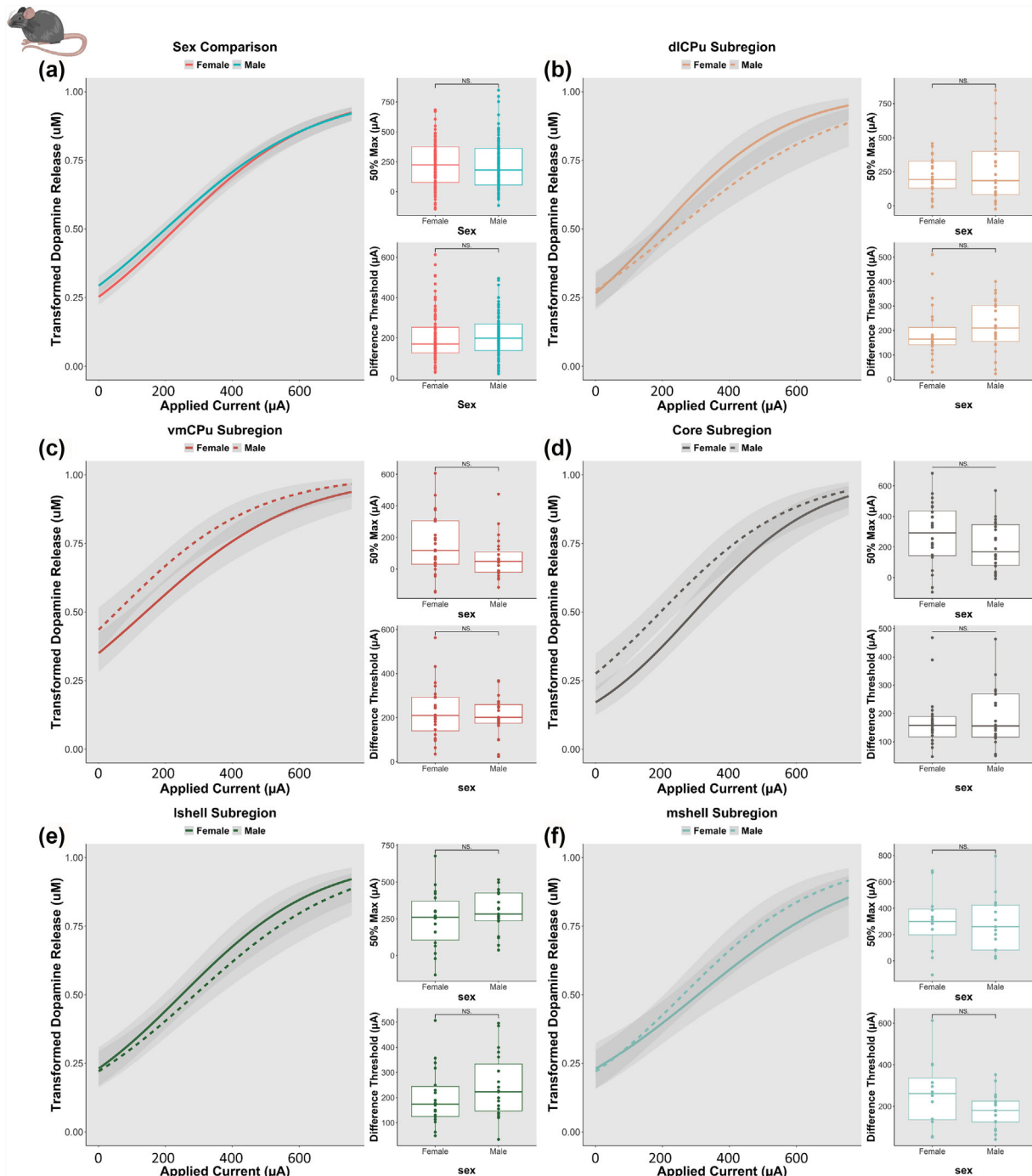


**FIGURE 5** Stimulus intensity response curves comparing transformed dopamine (DA) release of mice for each applied current. (a) Stimulus intensity response curve compared by sex for all mice with 50% Max calculation and difference threshold for each sex based on stimulus intensity response curve. (b) For dorsolateral caudate putamen (dlCPu) subregion. (c) For ventromedial caudate putamen (vmCPu) subregion. (d) For nucleus accumbens core (core) subregion. (e) For nucleus accumbens lateral shell (lshell) subregion. (f) For nucleus accumbens medial shell (mshell) subregion. \* $p < 0.05$ ; \*\* $p < 0.01$ ; \*\*\* $p < 0.001$ .

curves (Figure 6d). However, female caudal curves did have significantly different DTs across the subregions (Figure 6f;  $F(4,38) = 3.592, p = 0.014$ ), with a post-hoc pairwise *t*-test revealing the following individual differences: vmCPu versus mshell ( $p = 0.010$ ); dlCPu versus mshell ( $p = 0.015$ ); core versus mshell ( $p = 0.034$ ). Each

subregion was also broken down within sex into rostral and caudal curves to determine if the z-plane significantly affected 50% Max or DT (Figure S3). The only regions that displayed an effect of the z-plane were the mshell in males, with a significant difference in DT ( $F(1,16) = 7.306, p = 0.0157$ ; Figure S3I), and the dlCPu in

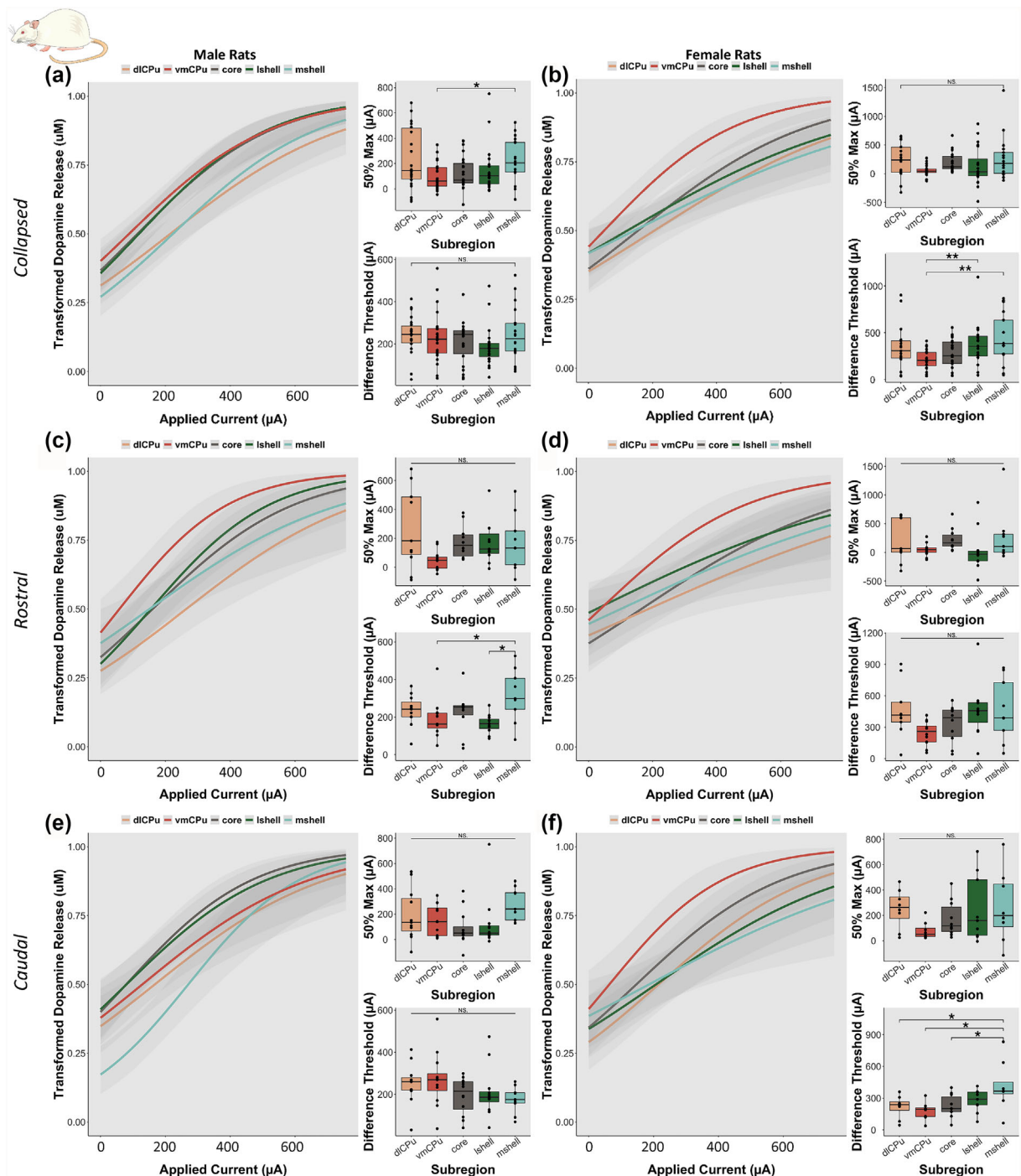


**FIGURE 6** Stimulus intensity response curves comparing transformed dopamine (DA) release of rats for each applied current between subregions. (a) Stimulus intensity response curve by subregion for male rats collapsed across z-plane (rostral and caudal) with 50% Max calculation and difference threshold for each subregion based on stimulus intensity response curve for male rats collapsed across z-plane. (b) For female rats collapsed across z-plane. (c) For male rats rostral z-plane only. (d) For female rats rostral z-plane only. (e) For male rats caudal z-plane only. (f) For female rats caudal z-plane only. core, nucleus accumbens core; dlCPu, dorsolateral caudate putamen; lshell, nucleus accumbens lateral shell; mshell, nucleus accumbens medial shell; vmCPu, ventromedial caudate putamen. \* $p < 0.05$ ; \*\* $p < 0.01$ .

females, which had a significant difference in DT ( $F(1,15) = 5.878, p = 0.0284$ ; Figure S3B).

The rat SIR curves were further compared by sex in Figure 7. All subregions were combined (Figure 7a) to

provide an overall sex comparison and a significant difference in the DT was found ( $F(1,200) = 21.07, p = 7.81 \times 10^{-6}$ ). When comparing individual subregions by sex, the only regions that displayed significant sex effects

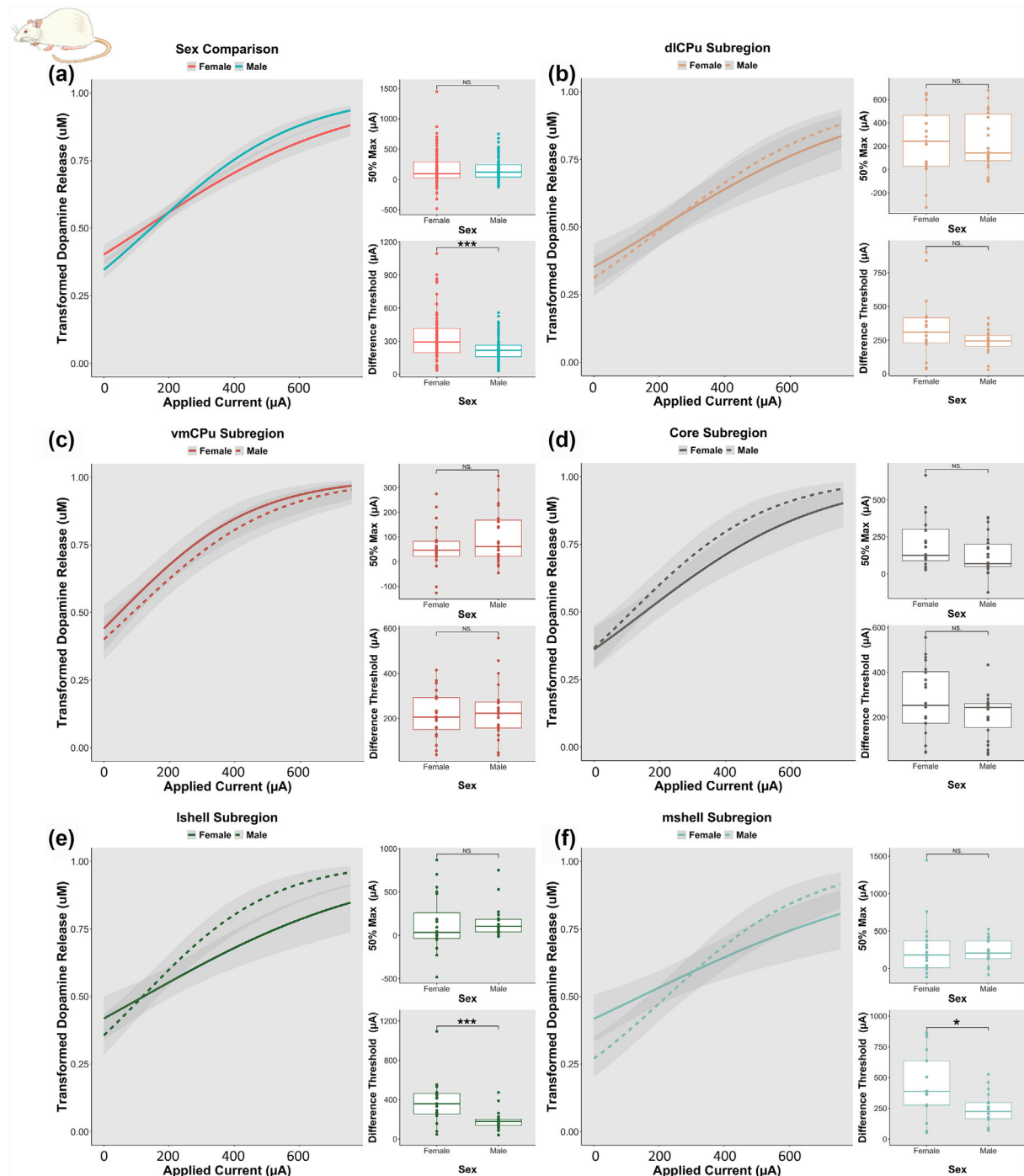


**FIGURE 7** Stimulus intensity response curves comparing transformed dopamine (DA) release of rats for each applied current. (a) Stimulus intensity response curve compared by sex for all rats with 50% Max calculation and difference threshold for each sex based on stimulus intensity response curve. (b) For dorsolateral caudate putamen (dlCPu) subregion. (c) For ventromedial caudate putamen (vmCPu) subregion. (d) For nucleus accumbens core (core) subregion. (e) For nucleus accumbens lateral shell (lshell) subregion. (f) For nucleus accumbens medial shell (mshell) subregion. \* $p < 0.05$ ; \*\* $p < 0.01$ ; \*\*\* $p < 0.001$ .

were the lshell DT (Figure 7e;  $p = 0.0005$ ) and the mshell DT (Figure 7f;  $p = 0.019$ ). Additionally, curves from individual subregions were also broken down by z-plane and compared (Figure S4), with sex differences discovered in DT in the following subregions: rostral dlCPu

( $p = 0.0074$ ; Figure S4A), rostral lshell ( $p = 0.0008$ ; Figure S4G) and caudal mshell ( $p = 0.0079$ ; Figure S4J).

SIR curve analysis in the rats revealed a higher DT in females than males across subregions, with the exception of vmCPu, which was the lowest of the subregions in

females. Subregion and sex differences in SIR curve outcomes were not consistent across species.

## 4 | DISCUSSION

Here, we describe a systematic ex vivo FSCV study of DA dynamics across multiple striatal subregions of male and female rats and mice. The results of our study reveal a more nuanced topography than what has been previously described as a simple dorsoventral gradient of DA release and uptake in the rodent striatum. Additionally, an analysis of the relationship between release and uptake is presented for each target subregion of interest, including dlCPu, vmCPu, NAc core, lshell and mshell. Finally, we explore ways to interpret the nonlinear relationship between applied stimulation current and resulting recorded DA release.

Understanding the precise function and behavioural significance of the subregions comprising the striatum is continually evolving. For details on the current understanding of the functional connectivity of all the brain regions surveyed in our study, we direct the reader to extensive and detailed reviews on the subject (Castro & Bruchas, 2019; de Jong et al., 2022; Garritsen et al., 2023). It is worthwhile, however, to at least outline the major functions of each of the five subregions from which we measured. The dlCPu is robustly connected with motor and premotor cortices (Voorn et al., 2004), and this region integrates sensorimotor input to facilitate control of voluntary movement. The vmCPu is involved in the processing of reward but with greater involvement in habit formation and the execution of well-learned actions. The NAc core plays a major role in reinforcement learning via encoding of signals integrated from both the novelty and saliency of a stimulus, termed ‘perceived saliency’ (Kutlu et al., 2021). The NAc shell can be divided into the medial and lateral portions, both of which, like the core, are involved in motivation and reward processing. The lshell has often been neglected when investigating the function of the NAc shell, but recent research suggests the medial and lshell have opposing motivational roles. Prior studies have shown that lshell neurons are primarily activated by the consumption of a reward, while mshell neurons decrease activity upon reward consumption (Bond et al., 2020; Chen et al., 2023). This prior study also demonstrated that the function of each of these two regions is continually refined by cue-associated learning via the recruitment of more neurons with excitatory response in the lshell and more neurons with inhibitory responses in the mshell. The opposing roles in behaviour are further supported by distinct gene expression between and diverse inputs to

these two subregions. Interestingly, the lshell inputs more closely resemble those of the core in both structure and function. Conversely, the mshell is one of the most enigmatic areas of the mesocorticolimbic system where the ‘functional logic’ that dictates the rest of the system appears to be reversed (Castro & Bruchas, 2019). Unique to the mshell, efferents from this region are positioned to directly inhibit ventral tegmental area (VTA) DA neurons; this direct signalling predominates the indirect (disinhibiting) connectivity that parallels that of lshell efferents to VTA (Yang et al., 2018). Additionally, the mshell integrates a remarkable variety of neuropeptidergic afferents, including direct inputs from the lateral hypothalamus (Castro & Bruchas, 2019).

More generally, the rodent striatum is traditionally divided into dorsal (caudate putamen, CPu) and ventral (NAc) compartments. Functionally, while there is some overlap, the CPu regulates motor processing and the NAc is involved in motivation and reward learning. Early labelling studies found greater DAT expression and faster DA clearance in the dorsal striatum compared with ventral areas (Cass et al., 1992; Sesack et al., 1998). Our study demonstrates that the more dorsal subregions generally exhibited the highest DA release and fastest uptake rates, in contrast with generally lower release and uptake in the two most ventral subregions (lateral and medial NAc shell). This is consistent with previous studies in males (Calipari et al., 2012) and the present work extends this finding to females. Interestingly, in freely-moving mice, phasic DA signals in the dorsal striatum are much smaller than those in the ventral striatum (Willuhn et al., 2012, 2014). This suggests that, as measured in the present study, ex vivo DA signalling in ventral subregions, stimulated with single pulses, does not reflect the full capacity of those regions to release DA; an observation that is supported by earlier ex vivo FSCV work (Zhang et al., 2009). A promising new method for monitoring rapid DA changes, including in freely-moving animals, involves the application of fluorescent sensors (e.g., dLight) alongside photometric recording (Delaney et al., 2024; Mohebi et al., 2023; Patriarchi et al., 2018; Salinas et al., 2023; Sun et al., 2018). This technique allows researchers to monitor DA signalling in the mesolimbic system during voluntary behaviour, without confounds associated with applying electrical stimulation to DA terminals, such as the concurrent release of acetylcholine in ex vivo FSCV (discussed more below).

There is considerable evidence in the literature of rostro-caudal differences in neural structure and function within the striatum. Within the conventional striatal subdivisions (CPu, NAc core and NAc shell), afferent/efferent connectivity and local synaptic structure vary along the rostro-caudal axis (Gangarossa et al., 2013;

Mennicken et al., 1992; Usuda et al., 1998), with observable functional variation. For example, it appears that the inhibitory influence of kappa opioid receptors on DA release is more pronounced in the caudal than rostral NAc core (Karkhanis et al., 2023) and shell (Pirino et al., 2020). In numerous studies, opposing behavioural responses have been observed upon applying chemogenetic and optogenetic activation/inhibition to rostral versus caudal NAc subregions (Hamel et al., 2017; Hurley et al., 2017; Kawashima et al., 2023). In the present study, significant rostro-caudal differences in single-pulse evoked DA release were observed in the vmCPU of male mice and the vmCPU and core of male rats (higher release in caudal slices). Rostro-caudal differences in DA uptake were not found, though a trend towards higher uptake in the rostral core of male mice was observed ( $p = 0.1267$ ). It is worth noting that the rostro-caudal difference in release in vmCPU was observed in males of both species but not females. Further study of this finding is warranted to investigate the possibility of sexual dimorphism.

There are notable sex differences in the regulation of DAergic transmission, reviewed in Zachry et al. (2021). One study demonstrated that both DA release and uptake, as measured by FSCV, were greater in females than in males (Walker et al., 2000). In our study, female mice generally exhibited an increased uptake rate compared with males, while female rats exhibited decreased DA release (a similar, but not significant, trend was seen in the mice). An important methodological consideration in the present study that may account for the discrepancy with prior findings is that, in the present study, placement selection did not depend on the robustness of DA signals. In the prior studies, it was important to choose high-release locations to ensure the ability to detect small changes and to maintain measurable signals after application of release-inhibiting drugs. In contrast, the present study design did not exclude less robust signals, thus capturing the lower end of the distribution as well as the upper, with the goal of providing more complete sets of observations. Although this aspect of data collection may have limited the ability to detect sex differences in release and uptake due to the range of signals included, measures such as the ratio of release to uptake reflect the sex differences previously reported in the literature, as further explained below.

To expand our comparison of regulation of DA across the striatum we plotted the relationship between release and uptake in each region as a correlation fitted to a linear regression, thereby determining a ratio of release to uptake (Figure 3, Table 6). DA release-to-uptake ratios have been used for evaluating the DA system since the early days of FSCV research (Garris & Wightman, 1994).

When the release and uptake rates are balanced, the system is considered to be in a ‘steady-state’ (Wightman et al., 1988). Because DA evoked by single pulses is not impacted by autoreceptor function in slices, the electrical stimulation used within the present experiments causes DA release to exceed that of the uptake, resulting in a loss of ‘steady-state’. The ratio provides useful information regarding the relative release sites to transporters’ expression within the measurement area, with a small ratio of release to uptake considered an ‘uptake dominated’ system, while a large release to uptake ratio is considered ‘release dominated’. The aim of our investigation was to shed new light on DA kinetics in the subcompartments within the striatum, in particular how these differed across species and sex. For instance, rats generally demonstrated lower ratios than mice, indicating a greater uptake rate relative to release sites, confirming previous findings of rats having an uptake-dominated system (Calipari et al., 2012). The females of both species consistently exhibited lower ratios in each subregion compared with males (the only exception being the mshell of mice). This is useful as an observation especially given that comparing absolute values between sexes in uptake did not reveal sex differences in the rodents in the present study, the females still exhibited significantly lower ratios of release-to-uptake, consistent with the greater transporter expression and activity in females shown in the literature (Zachry et al., 2021). This increased DAT expression and activity is posited to underlie sex differences in the presentation of various psychiatric disorders (Williams et al., 2021).

Another feature of these experiments is that electrically evoked DA in brain slices varies non-linearly as a function of applied stimulation current. As the stimulation current increases, a wider field of DA terminals is engaged (Mohammad Mahdi Alavi et al., 2021). DA release-promoting nicotinic acetylcholine receptors (nAChRs; further discussed below) are also engaged to a varying degree depending on stimulus intensity, likely playing a role in the non-linearity of the stimulus-release function. Importantly, all our ‘baseline’ DA measurements (Figures 1 and 2) were taken upon application of single-pulse stimulation at an intensity of 700  $\mu$ A, which is relatively high, resulting in peri-maximal DA release for brain slice recordings. Other studies employ lower stimulation intensities (250–350  $\mu$ A) according to the experimental need (Liu et al., 2022; O’Neill et al., 2017; Siciliano et al., 2015). Our lab and others have explored different ways to analyse and interpret the dynamic interaction between stimulus intensity and evoked DA. Here, we have used methods typically applied in other subfields of neuroscience, such as electrophysiology, to our FSCV data. Stimulus intensity response (SIR) curves

(Figures 4–7) display the peak amount of DA release on a logistic scale at each given current intensity, and they provide quantitative measures of how electrically evoked DA release varies at the level of individual slices. For simplicity, we have limited our analysis to include the measures of current required to reach 50% of the maximal DA response, here termed ‘50% Max’, and the smallest applied current required to elicit a detectable DA response, here termed the ‘difference threshold’ (DT). Changes in the 50% Max can be visualized by a right or left shift in the curve, with a left shift in the curve meaning a lower applied current is necessary to reach 50% maximum DA release (lower 50% Max), whereas a right shift would mean a higher applied current is needed (higher 50% Max). Interestingly, while two subregions (for example, vmCPu and lshell in male rats) may require a similar applied current to release half of their respective maximum output, it does not necessarily mean that those maximums are the same, as these calculations are derived after the curves have been transformed. The DT can be visualized as the steepness of the slope of the curve. A steeper curve would mean larger changes in incremental DA release across the tested stimulation currents (lower DT), whereas a flatter curve would mean smaller incremental DA release changes across the same stimulation currents (higher DT). A steeper curve/lower DT may reflect a greater ‘dynamic range’ of responses to varying stimulation currents and, thus, a greater ability of DA synapses to meet various physiological demands. This property of the DA system is thought to be exploited in the development of maladaptive behaviours, as observed in the failure to avoid aversive stimuli in substance use disorder (Thibeault et al., 2019). Finally, these data are intended to be used for future work to help aid in the selection of applied stimulation currents in baseline comparisons, as they help determine the stimulation necessary to evoke meaningful changes in DA release.

SIR curves have the potential to describe numerous features of DA terminals, including readily releasable pool capacity and the density of active-zone-like release sites (Liu et al., 2021). The present data show, as an example, that the vmCPu in male mice requires lower stimulation to reach 50% Max DA release compared with other subregions in males (Figure 4a), while the caudal mshell in female rats has slower and smaller incremental DA release (higher DT) than other caudal subregions in females (Figure 6f). While both results suggest differences in DA release in these subregions, the quantitative measures from SIR curves may help disentangle the differences in DA release dynamics across species and between sexes. These results also may provide evidence that the vmCPu in male mice engages a greater proportion of

available active sites for DA release across a broad range of applied stimulation currents, whereas the vmCPu in female rats appears to be more easily induced to release DA at very low applied stimulation currents, which could indicate a greater density of available active sites. All possible comparisons that can be made from the SIR curves within this dataset are too numerous to discuss in detail, but we provide these examples to demonstrate the utility of SIR curve analyses.

A mechanism that may contribute to the regional variability in SIR curve characteristics is the cholinergic system. Throughout the striatum, DA release is enhanced by the activation of nAChRs containing the  $\beta 2$  subunit upon acetylcholine release from nearby cholinergic interneurons (CINs; (Brimblecombe et al., 2018; Cragg, 2006; Rice & Cragg, 2004). The electrical stimulation used in the present study to evoke DA release also evokes the concurrent release of acetylcholine from CIN terminals, which augments the release of DA. This is evidenced in prior work by the marked reduction in measured DA release in slices upon application of a nAChR (Brimblecombe et al., 2018). The present study was not conducted in the presence of a nAChR antagonist, thus it cannot be ruled out that regional and sex differences in DA measures, including SIR curve measures, could depend on the cholinergic activity.

Two well-studied biological rhythms are known to influence DA regulation: the estrous cycle in females (Miller et al., 2023; Shanley et al., 2023; Zachry et al., 2021) and diurnal rhythms in rodents of both sexes (Jameson et al., 2023; Webb et al., 2015). DAergic activity is also influenced by the brain’s circadian clock (Fifel et al., 2018), and behaviours known to be modulated by DA are most prominent in rodents’ dark (awake) period. Because measurements in the present study were taken during the light period, interpretations related to awake behaviours should be made while considering this caveat.

In line with recent efforts to strengthen the scientific record through FAIR (findable, accessible, interoperable, reusable) data principles (Thorp et al., 2023; Wilkinson et al., 2016), the dataset from this study is stored Dryad data repository (<https://datadryad.org>) and is openly available for use in research. The data included in the repository are raw data and, thus, can be analysed using other mathematical models. While additional powerful techniques have been developed and used to aid in reaching a more complete understanding of DA neurotransmission and resulting downstream modulation of cellular activity, ex vivo FSCV remains an important tool for capturing information about regulatory actions at the DA terminal. FSCV elucidates synaptic regulation of DA dynamics and the influence of different genetic,

stress and drug exposure models on the DA system (Ferris, Calipari, Yorgason, & Jones, 2013). Our laboratory and others have shown that alterations observed in voltammetric measurements reflect neuroplasticity, including altered innervation density and receptor and transporter expression (Abdalla et al., 2020; Singer et al., 2016; van Elzelingen et al., 2022). Furthermore, studies have linked these functional changes with behavioural adaptations (Singer et al., 2016; van Elzelingen et al., 2022). The present dataset is available as a resource for future inquiries seeking to connect behavioural observations with variations in the striatal DA system.

## AUTHOR CONTRIBUTIONS

**Lindsey B. Kuiper:** Conceptualization; data curation; formal analysis; investigation; methodology; project administration; validation; visualization; writing—original draft; writing—review and editing. **Monica H. Dawes:** Conceptualization; data curation; formal analysis; investigation; validation; visualization; writing—review and editing. **Alyssa M. West:** Conceptualization; data curation; formal analysis; investigation; validation; visualization; writing—original draft; writing—review and editing. **Emily K. DiMarco:** Data curation; formal analysis; investigation; methodology; validation; visualization; writing—original draft; writing—review and editing. **Emma V. Galante:** Data curation; formal analysis; investigation; visualization. **Kenneth T. Kishida:** Funding acquisition; resources; supervision; writing—review and editing. **Sara R. Jones:** Conceptualization; funding acquisition; project administration; resources; supervision; visualization; writing—review and editing.

## ACKNOWLEDGEMENTS

We thank Dr. Katie Holleran for providing useful feedback on the manuscript. The National Institute on Drug Abuse (NIDA) funded this study through award numbers R01 DA048096 (KTK), P50 DA006634 (KTK), T32 DA041349 (SRJ), R01 DA048490 (SRJ), R01 DA054694 (SRJ), P50 DA006634 (SRJ), F31 DA057815 (MHD) and T32 DA041349 (MHD). The National Institute on Alcohol Abuse and Alcoholism (NIAAA) funded this study through award numbers P50 AA026117 (KTK), T32 AA007565 (AMW, LBK) and U01 AA014091 (SRJ). The National Institute of Mental Health funded this study through award numbers R01 MH121099 (KTK) and R01 MH124115 (KTK). The National Center for Advancing Translational Sciences funded this study through award number KL2 TR001420 (KTK). The content is solely the responsibility of the authors and does not necessarily represent the official views of the National Institutes of Health.

## CONFLICT OF INTEREST STATEMENT

The authors declare no conflict of interest.

## PEER REVIEW

The peer review history for this article is available at <https://www.webofscience.com/api/gateway/wos/peer-review/10.1111/ejn.16495>.

## DATA AVAILABILITY STATEMENT

The data that support the findings of this study are openly available in the Dryad data repository at 10.5061/dryad.sf7m0cgcn.

## ORCID

- Lindsey B. Kuiper  <https://orcid.org/0000-0002-0268-5133>
- Monica H. Dawes  <https://orcid.org/0000-0002-4729-5526>
- Emily K. DiMarco  <https://orcid.org/0000-0003-2950-4395>
- Kenneth T. Kishida  <https://orcid.org/0000-0002-7394-8922>
- Sara R. Jones  <https://orcid.org/0000-0002-3424-7576>

## REFERENCES

- Abdalla, A., West, A., Jin, Y., Saylor, R. A., Qiang, B., Pena, E., Linden, D. J., Nijhout, H. F., Reed, M. C., Best, J., & Hashemi, P. (2020). Fast serotonin voltammetry as a versatile tool for mapping dynamic tissue architecture: I. Responses at carbon fibers describe local tissue physiology. *Journal of Neurochemistry*, 153(1), 33–50. <https://doi.org/10.1111/jnc.14854>
- Bond, C. W., Trinko, R., Foscue, E., Furman, K., Groman, S. M., Taylor, J. R., & DiLeone, R. J. (2020). Medial nucleus accumbens projections to the ventral tegmental area control food consumption. *The Journal of Neuroscience*, 40(24), 4727–4738. <https://doi.org/10.1523/JNEUROSCI.3054-18.2020>
- Brimblecombe, K. R., Threlfell, S., Dautan, D., Kosillo, P., Mena-Segovia, J., & Cragg, S. J. (2018). Targeted activation of cholinergic interneurons accounts for the modulation of dopamine by striatal nicotinic receptors. *eNeuro*, 5(5), ENEURO.0397-17.2018. <https://doi.org/10.1523/ENEURO.0397-17.2018>
- Budygin, E. A., Oleson, E. B., Mathews, T. A., Lack, A. K., Diaz, M. R., McCool, B. A., & Jones, S. R. (2007). Effects of chronic alcohol exposure on dopamine uptake in rat nucleus accumbens and caudate putamen. *Psychopharmacology*, 193(4), 495–501. <https://doi.org/10.1007/s00213-007-0812-1>
- Calipari, E. S., Huggins, K. N., Mathews, T. A., & Jones, S. R. (2012). Conserved dorsal-ventral gradient of dopamine release and uptake rate in mice, rats and rhesus macaques. *Neurochemistry International*, 61(7), 986–991. <https://doi.org/10.1016/j.neuint.2012.07.008>
- Cass, W. A., Gerhardt, G. A., Mayfield, R. D., Curella, P., & Zahniser, N. R. (1992). Differences in dopamine clearance and diffusion in rat striatum and nucleus accumbens following systemic cocaine administration. *Journal of Neurochemistry*,

- 59(1), 259–266. <https://doi.org/10.1111/j.1471-4159.1992.tb0899.x>
- Castro, D. C., & Bruchas, M. R. (2019). A motivational and neuro-peptidergic hub: Anatomical and functional diversity within the nucleus accumbens shell. *Neuron*, 102(3), 529–552. <https://doi.org/10.1016/j.neuron.2019.03.003>
- Chen, G., Lai, S., Bao, G., Ke, J., Meng, X., Lu, S., Wu, X., Xu, H., Wu, F., Xu, Y., Xu, F., Bi, G. Q., Peng, G., Zhou, K., & Zhu, Y. (2023). Distinct reward processing by subregions of the nucleus accumbens. *Cell Reports*, 42(2), 112069. <https://doi.org/10.1016/j.celrep.2023.112069>
- Christiansen, D. M., McCarthy, M. M., & Seeman, M. V. (2022). Editorial: Understanding the influences of sex and gender differences in mental disorders. *Frontiers in Psychiatry*, 13, 984195. <https://doi.org/10.3389/fpsyg.2022.984195>
- Cora, M. C., Kooistra, L., & Travlos, G. (2015). Vaginal cytology of the laboratory rat and mouse: Review and criteria for the staging of the estrous cycle using stained vaginal smears. *Toxicologic Pathology*, 43(6), 776–793. <https://doi.org/10.1177/0192623315570339>
- Cragg, S. J. (2006). Meaningful silences: How dopamine listens to the ACh pause. *Trends in Neurosciences*, 29(3), 125–131. <https://doi.org/10.1016/j.tins.2006.01.003>
- de Jong, J. W., Fraser, K. M., & Lammel, S. (2022). Mesoaccumbal dopamine heterogeneity: What do dopamine firing and release have to do with it? *Annual Review of Neuroscience*, 45, 109–129. <https://doi.org/10.1146/annurev-neuro-110920-011929>
- Delaney, J., Nathani, S., Tan, V., Chavez, C., Orr, A., Paek, J., Faraji, M., Setlow, B., & Urs, N. M. (2024). Enhanced cognitive flexibility and phasic striatal dopamine dynamics in a mouse model of low striatal tonic dopamine. *Neuropsychopharmacology*. Advance online publication. <https://doi.org/10.1038/s41386-024-01868-5>
- Ferris, M. J., Calipari, E. S., Melchior, J. R., Roberts, D. C., Espana, R. A., & Jones, S. R. (2013). Paradoxical tolerance to cocaine after initial supersensitivity in drug-use-prone animals. *The European Journal of Neuroscience*, 38(4), 2628–2636. <https://doi.org/10.1111/ejn.12266>
- Ferris, M. J., Calipari, E. S., Yorgason, J. T., & Jones, S. R. (2013). Examining the complex regulation and drug-induced plasticity of dopamine release and uptake using voltammetry in brain slices. *ACS Chemical Neuroscience*, 4(5), 693–703. <https://doi.org/10.1021/cn400026v>
- Ferris, M. J., Espana, R. A., Locke, J. L., Konstantopoulos, J. K., Rose, J. H., Chen, R., & Jones, S. R. (2014). Dopamine transporters govern diurnal variation in extracellular dopamine tone. *Proceedings of the National Academy of Sciences of the United States of America*, 111(26), E2751–E2759. <https://doi.org/10.1073/pnas.1407935111>
- Fifel, K., Meijer, J. H., & Deboer, T. (2018). Circadian and homeostatic modulation of multi-unit activity in midbrain dopaminergic structures. *Scientific Reports*, 8(1), 7765. <https://doi.org/10.1038/s41598-018-25770-5>
- Floresco, S. B. (2007). Dopaminergic regulation of limbic-striatal interplay. *Journal of Psychiatry & Neuroscience*, 32(6), 400–411. <https://www.ncbi.nlm.nih.gov/pubmed/18043763>
- Gangarossa, G., Espallergues, J., Mailly, P., De Bundel, D., de Kerchove d'Exaerde, A., Herve, D., Girault, J. A., Valjent, E., & Krieger, P. (2013). Spatial distribution of D1R- and D2R-expressing medium-sized spiny neurons differs along the rostral-caudal axis of the mouse dorsal striatum. *Frontiers in Neural Circuits*, 7, 124. <https://doi.org/10.3389/fncir.2013.00124>
- Garris, P. A., Ciolkowski, E. L., & Wightman, R. M. (1994). Heterogeneity of evoked dopamine overflow within the striatal and striatoamygdaloid regions. *Neuroscience*, 59(2), 417–427. [https://doi.org/10.1016/0306-4522\(94\)90606-8](https://doi.org/10.1016/0306-4522(94)90606-8)
- Garris, P. A., & Wightman, R. M. (1994). Different kinetics govern dopaminergic transmission in the amygdala, prefrontal cortex, and striatum: An in vivo voltammetric study. *The Journal of Neuroscience*, 14(1), 442–450. <https://doi.org/10.1523/JNEUROSCI.14-01-00442.1994>
- Garritsen, O., van Battum, E. Y., Grossouw, L. M., & Pasterkamp, R. J. (2023). Development, wiring and function of dopamine neuron subtypes. *Nature Reviews Neuroscience*, 24(3), 134–152. <https://doi.org/10.1038/s41583-022-00669-3>
- George, B. E., Dawes, M. H., Peck, E. G., & Jones, S. R. (2022). Altered accumbal dopamine terminal dynamics following chronic heroin self-administration. *International Journal of Molecular Sciences*, 23(15), 8106. <https://doi.org/10.3390/ijms23158106>
- Gonzales, K. K., & Smith, Y. (2015). Cholinergic interneurons in the dorsal and ventral striatum: Anatomical and functional considerations in normal and diseased conditions. *Annals of the New York Academy of Sciences*, 1349(1), 1–45. <https://doi.org/10.1111/nyas.12762>
- Hamel, L., Thangarasa, T., Samadi, O., & Ito, R. (2017). Caudal nucleus accumbens core is critical in the regulation of cue-elicited approach-avoidance decisions. *eNeuro*, 4(1), ENEURO.0330-16.2017. <https://doi.org/10.1523/ENEURO.0330-16.2017>
- Hurley, S. W., West, E. A., & Carelli, R. M. (2017). Opposing roles of rapid dopamine signaling across the rostral-caudal axis of the nucleus accumbens shell in drug-induced negative affect. *Biological Psychiatry*, 82(11), 839–846. <https://doi.org/10.1016/j.biopsych.2017.05.009>
- Jameson, A. N., Siemann, J. K., Melchior, J., Calipari, E. S., McMahon, D. G., & Grueter, B. A. (2023). Photoperiod impacts nucleus accumbens dopamine dynamics. *eNeuro*, 10(2), ENEURO.0361-22.2023. <https://doi.org/10.1523/ENEURO.0361-22.2023>
- Jones, S. R., Garris, P. A., Kilts, C. D., & Wightman, R. M. (1995). Comparison of dopamine uptake in the basolateral amygdaloid nucleus, caudate-putamen, and nucleus accumbens of the rat. *Journal of Neurochemistry*, 64(6), 2581–2589. <https://doi.org/10.1046/j.1471-4159.1995.64062581.x>
- Jones, S. R., O'Dell, S. J., Marshall, J. F., & Wightman, R. M. (1996). Functional and anatomical evidence for different dopamine dynamics in the core and shell of the nucleus accumbens in slices of rat brain. *Synapse*, 23(3), 224–231. [https://doi.org/10.1002/\(SICI\)1098-2396\(199607\)23:3<224::AID-SYN12>3.0.CO;2-Z](https://doi.org/10.1002/(SICI)1098-2396(199607)23:3<224::AID-SYN12>3.0.CO;2-Z)
- Karkhanis, A. N., West, A. M., & Jones, S. R. (2023). Kappa opioid receptor agonist U50,488 inhibits dopamine more in caudal than rostral nucleus accumbens core. *Basic & Clinical Pharmacology & Toxicology*, 133(5), 526–534. <https://doi.org/10.1111/bcpt.13929>
- Kawashima, S., Lou, F., Kusumoto-Yoshida, I., Hao, L., & Kuwaki, T. (2023). Activation of the rostral nucleus accumbens shell by optogenetics induces cataplexy-like behavior in

- orexin neuron-ablated mice. *Scientific Reports*, 13(1), 2546. <https://doi.org/10.1038/s41598-023-29488-x>
- Kingdom, F. A. A., & Prins, N. (2016). *Psychophysics, a practical introduction* (2nd Edition). Academic Press.
- Kutlu, M. G., Zachry, J. E., Melugin, P. R., Cajigas, S. A., Chevée, M. F., Kelly, S. J., Kutlu, B., Tian, L., Siciliano, C. A., & Calipari, E. S. (2021). Dopamine release in the nucleus accumbens core signals perceived saliency. *Current Biology*, 31(21), 4748–4761.e8. <https://doi.org/10.1016/j.cub.2021.08.052>
- Liu, C., Goel, P., & Kaeser, P. S. (2021). Spatial and temporal scales of dopamine transmission. *Nature Reviews Neuroscience*, 22(6), 345–358. <https://doi.org/10.1038/s41583-021-00455-7>
- Liu, X., Vickstrom, C. R., Yu, H., Liu, S., Snarrenberg, S. T., Friedman, V., Mu, L., Chen, B., Kelly, T. J., Baker, D. A., & Liu, Q. S. (2022). Epac2 in midbrain dopamine neurons contributes to cocaine reinforcement via enhancement of dopamine release. *eLife*, 11, e80747. <https://doi.org/10.7554/eLife.80747>
- Lucio Boschen, S., Trevathan, J., Hara, S. A., Asp, A., & Lujan, J. L. (2021). Defining a path toward the use of fast-scan cyclic voltammetry in human studies. *Frontiers in Neuroscience*, 15, 728092. <https://doi.org/10.3389/fnins.2021.728092>
- Mennicken, F., Savasta, M., Peretti-Renucci, R., & Feuerstein, C. (1992). Autoradiographic localization of dopamine uptake sites in the rat brain with 3H-GBR 12935. *Journal of Neural Transmission. General Section*, 87(1), 1–14. <https://doi.org/10.1007/BF01253106>
- Miller, C. K., Krentzel, A. A., & Meitzen, J. (2023). ER $\alpha$  stimulation rapidly modulates excitatory synapse properties in female rat nucleus accumbens core. *Neuroendocrinology*, 113(11), 1140–1153. <https://doi.org/10.1159/000529571>
- Mohammad Mahdi Alavi, S., Goetz, S. M., & Saif, M. (2021). Input-output slope curve estimation in neural stimulation based on optimal sampling principles. *Journal of Neural Engineering*, 18(4), 046071. <https://doi.org/10.1088/1741-2552/abffe5>
- Mohebi, A., Collins, V. L., & Berke, J. D. (2023). Accumbens cholinergic interneurons dynamically promote dopamine release and enable motivation. *eLife*, 12, e85011. <https://doi.org/10.7554/eLife.85011>
- Mohebi, A., Pettibone, J. R., Hamid, A. A., Wong, J. T., Vinson, L. T., Patriarchi, T., Tian, L., Kennedy, R. T., & Berke, J. D. (2019). Dissociable dopamine dynamics for learning and motivation. *Nature*, 570(7759), 65–70. <https://doi.org/10.1038/s41586-019-1235-y>
- Nolan, S. O., Zachry, J. E., Johnson, A. R., Brady, L. J., Siciliano, C. A., & Calipari, E. S. (2020). Direct dopamine terminal regulation by local striatal microcircuitry. *Journal of Neurochemistry*, 155(5), 475–493. <https://doi.org/10.1111/jnc.15034>
- O'Neill, B., Patel, J. C., & Rice, M. E. (2017). Characterization of optically and electrically evoked dopamine release in striatal slices from digenic knock-in mice with DAT-driven expression of channelrhodopsin. *ACS Chemical Neuroscience*, 8(2), 310–319. <https://doi.org/10.1021/acscchemneuro.6b00300>
- Patriarchi, T., Cho, J. R., Merten, K., Howe, M. W., Marley, A., Xiong, W. H., Folk, R. W., Broussard, G. J., Liang, R., Jang, M. J., Zhong, H., Dombeck, D., von Zastrow, M., Nimmerjahn, A., Gradinaru, V., Williams, J. T., & Tian, L. (2018). Ultrafast neuronal imaging of dopamine dynamics with designed genetically encoded sensors. *Science*, 360(6396), eaat4422. <https://doi.org/10.1126/science.aat4422>
- Paxinos, G., & Watson, C. (2013). *The rat brain in stereotaxic coordinates* (7th Edition). Elsevier.
- Pirino, B. E., Spodnick, M. B., Gargiulo, A. T., Curtis, G. R., Barson, J. R., & Karkhanis, A. N. (2020). Kappa-opioid receptor-dependent changes in dopamine and anxiety-like or approach-avoidance behavior occur differentially across the nucleus accumbens shell rostro-caudal axis. *Neuropharmacology*, 181, 108341. <https://doi.org/10.1016/j.neuropharm.2020.108341>
- Rice, M. E., & Cragg, S. J. (2004). Nicotine amplifies reward-related dopamine signals in striatum. *Nature Neuroscience*, 7(6), 583–584. <https://doi.org/10.1038/nn1244>
- Rice, M. E., Patel, J. C., & Cragg, S. J. (2011). Dopamine release in the basal ganglia. *Neuroscience*, 198, 112–137. <https://doi.org/10.1016/j.neuroscience.2011.08.066>
- Roberts, J. G., Toups, J. V., Eyualem, E., McCarty, G. S., & Sombers, L. A. (2013). In situ electrode calibration strategy for voltammetric measurements in vivo. *Analytical Chemistry*, 85(23), 11568–11575. <https://doi.org/10.1021/ac402884n>
- Saddoris, M. P., Cacciapaglia, F., Wightman, R. M., & Carelli, R. M. (2015). Differential dopamine release dynamics in the nucleus accumbens core and shell reveal complementary signals for error prediction and incentive motivation. *The Journal of Neuroscience*, 35(33), 11572–11582. <https://doi.org/10.1523/JNEUROSCI.2344-15.2015>
- Salinas, A. G., Lee, J. O., Augustin, S. M., Zhang, S., Patriarchi, T., Tian, L., Morales, M., Mateo, Y., & Lovinger, D. M. (2023). Distinct sub-second dopamine signaling in dorsolateral striatum measured by a genetically-encoded fluorescent sensor. *Nature Communications*, 14(1), 5915. <https://doi.org/10.1038/s41467-023-41581-3>
- Sesack, S. R., Hawrylak, V. A., Matus, C., Guido, M. A., & Levey, A. I. (1998). Dopamine axon varicosities in the prelimbic division of the rat prefrontal cortex exhibit sparse immunoreactivity for the dopamine transporter. *The Journal of Neuroscience*, 18(7), 2697–2708. <https://doi.org/10.1523/JNEUROSCI.18-07-02697.1998>
- Shanley, M. R., Miura, Y., Guevara, C. A., Onoichenco, A., Kore, R., Ustundag, E., Darwish, R., Renzoni, L., Urbaez, A., Blicker, E., Seidenberg, A., Milner, T. A., & Friedman, A. K. (2023). Estrous cycle mediates midbrain neuron excitability altering social behavior upon stress. *The Journal of Neuroscience*, 43(5), 736–748. <https://doi.org/10.1523/JNEUROSCI.1504-22.2022>
- Siciliano, C. A., Calipari, E. S., Cuzon Carlson, V. C., Helms, C. M., Lovinger, D. M., Grant, K. A., & Jones, S. R. (2015). Voluntary ethanol intake predicts kappa-opioid receptor supersensitivity and regionally distinct dopaminergic adaptations in macaques. *The Journal of Neuroscience*, 35(15), 5959–5968. <https://doi.org/10.1523/JNEUROSCI.4820-14.2015>
- Singer, B. F., Guptaroy, B., Austin, C. J., Wohl, I., Lovic, V., Seiler, J. L., Vaughan, R. A., Gnegy, M. E., Robinson, T. E., & Aragona, B. J. (2016). Individual variation in incentive salience attribution and accumbens dopamine transporter expression and function. *The European Journal of Neuroscience*, 43(5), 662–670. <https://doi.org/10.1111/ejn.13134>
- Sun, F., Zeng, J., Jing, M., Zhou, J., Feng, J., Owen, S. F., Luo, Y., Li, F., Wang, H., Yamaguchi, T., Yong, Z., Gao, Y., Peng, W., Wang, L., Zhang, S., Du, J., Lin, D., Xu, M., Kreitzer, A. C., ... Li, Y. (2018). A genetically encoded fluorescent sensor enables

- rapid and specific detection of dopamine in flies, fish, and mice. *Cell*, 174(2), 481–496.e19. <https://doi.org/10.1016/j.cell.2018.06.042>
- Thibeault, K. C., Kutlu, M. G., Sanders, C., & Calipari, E. S. (2019). Cell-type and projection-specific dopaminergic encoding of aversive stimuli in addiction. *Brain Research*, 1713, 1–15. <https://doi.org/10.1016/j.brainres.2018.12.024>
- Thorp, H. H., Vinson, V., & Yeston, J. (2023). Strengthening the scientific record. *Science*, 380(6640), 13. <https://doi.org/10.1126/science.adj0333>
- Usuda, I., Tanaka, K., & Chiba, T. (1998). Efferent projections of the nucleus accumbens in the rat with special reference to subdivision of the nucleus: Biotinylated dextran amine study. *Brain Research*, 797(1), 73–93. [https://doi.org/10.1016/s0006-8993\(98\)00359-x](https://doi.org/10.1016/s0006-8993(98)00359-x)
- van Elzelingen, W., Goedhoop, J., Warnaar, P., Denys, D., Arbab, T., & Willuhn, I. (2022). A unidirectional but not uniform striatal landscape of dopamine signaling for motivational stimuli. *Proceedings of the National Academy of Sciences of the United States of America*, 119(21), e2117270119. <https://doi.org/10.1073/pnas.2117270119>
- Voorn, P., Vanderschuren, L. J., Groenewegen, H. J., Robbins, T. W., & Pennartz, C. M. (2004). Putting a spin on the dorsal-ventral divide of the striatum. *Trends in Neurosciences*, 27(8), 468–474. <https://doi.org/10.1016/j.tins.2004.06.006>
- Walker, Q. D., Rooney, M. B., Wightman, R. M., & Kuhn, C. M. (2000). Dopamine release and uptake are greater in female than male rat striatum as measured by fast cyclic voltammetry. *Neuroscience*, 95(4), 1061–1070. [https://doi.org/10.1016/s0306-4522\(99\)00500-x](https://doi.org/10.1016/s0306-4522(99)00500-x)
- Webb, I. C., Lehman, M. N., & Coolen, L. M. (2015). Diurnal and circadian regulation of reward-related neurophysiology and behavior. *Physiology & Behavior*, 143, 58–69. <https://doi.org/10.1016/j.physbeh.2015.02.034>
- Wightman, R. M., Amatore, C., Engstrom, R. C., Hale, P. D., Kristensen, E. W., Kuhr, W. G., & May, L. J. (1988). Real-time characterization of dopamine overflow and uptake in the rat striatum. *Neuroscience*, 25(2), 513–523. [https://doi.org/10.1016/0306-4522\(88\)90255-2](https://doi.org/10.1016/0306-4522(88)90255-2)
- Wilkinson, M. D., Dumontier, M., Aalbersberg, I. J., Appleton, G., Axton, M., Baak, A., Blomberg, N., Boiten, J. W., da Silva Santos, L. B., Bourne, P. E., Bouwman, J., Brookes, A. J., Clark, T., Crosas, M., Dillo, I., Dumon, O., Edmunds, S., Evelo, C. T., Finkers, R., & Mons, B. (2016). The FAIR Guiding Principles for scientific data management and stewardship. *Scientific Data*, 3(1), 160018. <https://doi.org/10.1038/sdata.2016.18>
- Williams, O. O. F., Coppolino, M., George, S. R., & Perreault, M. L. (2021). Sex differences in dopamine receptors and relevance to neuropsychiatric disorders. *Brain Sciences*, 11(9), 1199. <https://doi.org/10.3390/brainsci11091199>
- Willuhn, I., Burgeno, L. M., Everitt, B. J., & Phillips, P. E. (2012). Hierarchical recruitment of phasic dopamine signaling in the striatum during the progression of cocaine use. *Proceedings of the National Academy of Sciences of the United States of America*, 109(50), 20703–20708. <https://doi.org/10.1073/pnas.1213460109>
- Willuhn, I., Burgeno, L. M., Groblewski, P. A., & Phillips, P. E. (2014). Excessive cocaine use results from decreased phasic dopamine signaling in the striatum. *Nature Neuroscience*, 17(5), 704–709. <https://doi.org/10.1038/nn.3694>
- Yang, H., de Jong, J. W., Tak, Y., Peck, J., Bateup, H. S., & Lammel, S. (2018). Nucleus accumbens subnuclei regulate motivated behavior via direct inhibition and disinhibition of VTA dopamine subpopulations. *Neuron*, 97(2), 434–449.e4. <https://doi.org/10.1016/j.neuron.2017.12.022>
- Zachry, J. E., Nolan, S. O., Brady, L. J., Kelly, S. J., Siciliano, C. A., & Calipari, E. S. (2021). Sex differences in dopamine release regulation in the striatum. *Neuropsychopharmacology*, 46(3), 491–499. <https://doi.org/10.1038/s41386-020-00915-1>
- Zhang, L., Doyon, W. M., Clark, J. J., Phillips, P. E., & Dani, J. A. (2009). Controls of tonic and phasic dopamine transmission in the dorsal and ventral striatum. *Molecular Pharmacology*, 76(2), 396–404. <https://doi.org/10.1124/mol.109.056317>

## SUPPORTING INFORMATION

Additional supporting information can be found online in the Supporting Information section at the end of this article.

**How to cite this article:** Kuiper, L. B., Dawes, M. H., West, A. M., DiMarco, E. K., Galante, E. V., Kishida, K. T., & Jones, S. R. (2024). Comparison of dopamine release and uptake parameters across sex, species and striatal subregions. *European Journal of Neuroscience*, 60(6), 5113–5140. <https://doi.org/10.1111/ejn.16495>